

UNCLASSIFIED

AD NUMBER

AD859982

LIMITATION CHANGES

TO:

Approved for public release; distribution is unlimited.

FROM:

Distribution authorized to U.S. Gov't. agencies and their contractors; Critical Technology; JUN 1969. Other requests shall be referred to Naval Weapons Center, China Lake, CA. This document contains export-controlled technical data.

AUTHORITY

USNWC ltr dtd 24 Mar 1972

THIS PAGE IS UNCLASSIFIED

AD 859982

**COMBUSTION OF SOLID PROPELLANTS AND LOW
FREQUENCY COMBUSTION INSTABILITY PROGRESS REPORT
1 OCTOBER 1967--1 NOVEMBER 1968**

by

T. L. Boggs
H. B. Mathes
E. W. Price
K. J. Kraeutle
G. L. Dehority
J. E. Crump
F. E. C. Culick

DDC
RECEIVED
OCT 10 1969
RECEIVED

Research Department

ABSTRACT. This report summarizes studies of ammonium perchlorate deflagration; one-dimensional modeling of steady-state burning; burning rate behavior of propellants with bimodal oxidizer particle size distribution; burning surface structure; and mechanism of metal agglomeration on burning surfaces. A review is presented of the status of knowledge of bulk mode instability. Brief summaries are presented of other recently published work, including (1) extension of one-dimensional combustion perturbation models to treat transient gas phase response, (2) collection of response function data from three different experimental techniques to present a full range map of μ/ϵ versus p and f for propellants, and (3) further experimental studies of the structure of the combustion zone.



NAVAL WEAPONS CENTER
CHINA LAKE, CALIFORNIA • JUNE 1969

DISTRIBUTION STATEMENT

THIS DOCUMENT IS SUBJECT TO SPECIAL EXPORT CONTROLS AND EACH TRANSMITTAL TO FOREIGN GOVERNMENTS OR FOREIGN NATIONALS MAY BE MADE ONLY WITH PRIOR APPROVAL OF THE NAVAL WEAPONS CENTER.

**Best
Available
Copy**

1. INTRODUCTION

The research summarized in this report is a continuation of that reported earlier (Ref. 1-11). The primary objective is to understand and learn how to control combustion instability in solid rocket motors, especially in the low frequency range (up to about 500 cps). This objective was stimulated by the increasing interest in very large booster motors and low L* space motors. Laboratory tests and theoretical considerations indicated a significant risk of low frequency instability, and the impact of such problems on development programs promised to be very costly unless better laboratory tests and understanding of the phenomenon were available.

Preliminary studies were concerned with development of several laboratory techniques for the study of low frequency instability (LFI), and use of these methods to screen the effect of propellant variables on LFI (Ref. 1-4). This work provided a preliminary basis for assessment of the LFI problem in rocket motors, and provided experimental methods that could be applied when problems arose in development programs. However, it became evident that an adequate approach to the LFI problem was dependent on a better understanding of the detailed aspects of propellant combustion, and several studies (Ref. 4-7) were initiated which were of a more fundamental nature, related to ingredient decomposition, combustion zone structure, and acoustic attenuation processes (Ref 8-10). These studies were continued along with the LFI studies.

The fundamental studies included decomposition of ammonium perchlorate (AP) by differential thermal analysis (DTA) and by observation of nucleation and spread of decomposition sites on large, single, high purity crystals; observation of AP deflagration by high speed photography and study of quenched samples of large single crystals; study of combustion zone structure by photography and quenching of "sandwiches" of AP and binder; photographic observation of accumulation, agglomeration and combustion of powdered metal fuels in propellant combustion; hot plate heating and agglomeration mechanism of metals, and cold flow studies of acoustic attenuation in model combustors. These areas of research have been presented extensively in previous reports and publications. During the past year it has been necessary to drop some of these areas of investigation due to reductions in funding. Specifically, work in the following areas was dropped or transferred to other programs: AP decomposition, "sandwich burning", and experimental work on acoustic attenuation. The areas of continuing effort are indicated by the section headings in the report.

NOMENCLATURE

- A Nondimensional parameter, $\frac{E_s}{RT_s} \left(1 - \frac{T_o}{T_s}\right)$
- s Parameter in the granular diffusion flame correlation $p/r = a+bp^{2/3}$
- B Nondimensional parameter $\left(\frac{E_s}{RT_s} - 1/2\right) \left(1 - \frac{T_o}{T_s}\right)$
- b Parameter in the granular diffusion flame correlation $p/r = a+bp^{2/3}$
- c* Effective discharge velocity of nozzle
- E_s Activation energy of solid
- L* Volume of chamber/area of nozzle throat
- m Mass burning rate
- n Pressure exponent from $r = Cp^n$
- p Pressure
- R Magnitude of combustion response to pressure disturbance,
 $R = (m/\bar{m}) / (p/\bar{p})$
- r Burning rate
- α Growth rate of pressure oscillations
- Γ "Constant" value between 1 and $(r+1)/2r$, depending on extent of temperature oscillation in combustor
- κ Thermal diffusivity
- λ Characteristic root of solid phase energy
- w/ϵ Ratio of mass perturbation to pressure perturbation. Also designated the propellant response function
- τ Time lead of combustion oscillation relative to perturbing pressure oscillation

◆ "Constant", value between $(1/r) [2/(r+1)]^{-\frac{r+1}{r-1}}$ and $(1/r)^2 [2/(r+1)]^{-\frac{r+1}{r-1}}$

Ω Ω = $\kappa\omega/\bar{r}^2$

ω Frequency of oscillation, rad/aec

SUBSCRIPT

s Solid

o Total

SUPERSCRIPIT

- Time averaged value

/ Perturbation

BLANK PAGE

1. INTRODUCTION

The research summarized in this report is a continuation of that reported earlier (Ref. 1-11). The primary objective is to understand and learn how to control combustion instability in solid rocket motors, especially in the low frequency range (up to about 500 cps). This objective was stimulated by the increasing interest in very large booster motors and low L^* space motors. Laboratory tests and theoretical considerations indicated a significant risk of low frequency instability, and the impact of such problems on development programs promised to be very costly unless better laboratory tests and understanding of the phenomenon were available.

Preliminary studies were concerned with development of several laboratory techniques for the study of low frequency instability (LFI), and use of these methods to screen the effect of propellant variables on LFI (Ref. 1-4). This work provided a preliminary basis for assessment of the LFI problem in rocket motors, and provided experimental methods that could be applied when problems arose in development programs. However, it became evident that an adequate approach to the LFI problem was dependent on a better understanding of the detailed aspects of propellant combustion, and several studies (Ref. 4-7) were initiated which were of a more fundamental nature, related to ingredient decomposition, combustion zone structure, and acoustic attenuation processes (Ref 8-10). These studies were continued along with the LFI studies.

The fundamental studies included decomposition of ammonium perchlorate (AP) by differential thermal analysis (DTA) and by observation of nucleation and spread of decomposition sites on large, single, high purity crystals; observation of AP deflagration by high speed photography and study of quenched samples of large single crystals; study of combustion zone structure by photography and quenching of "sandwiches" of AP and binder; photographic observation of accumulation, agglomeration and combustion of powdered metal fuels in propellant combustion; hot plate heating and agglomeration mechanism of metals, and cold flow studies of acoustic attenuation in model combustors. These areas of research have been presented extensively in previous reports and publications. During the past year it has been necessary to drop some of these areas of investigation due to reductions in funding. Specifically, work in the following areas was dropped or transferred to other programs: AP decomposition, "sandwich burning", and experimental work on acoustic attenuation. The areas of continuing effort are indicated by the section headings in the report.

Much of the work on the present program has seen publication in two or more forms, e.g., as progress reports, summary reports of particular areas of work, and as open literature publications. In the interests of economy, it was decided that the present report would present only brief resumes of those areas in which complete publication in some other form was available on a comparable time scale.

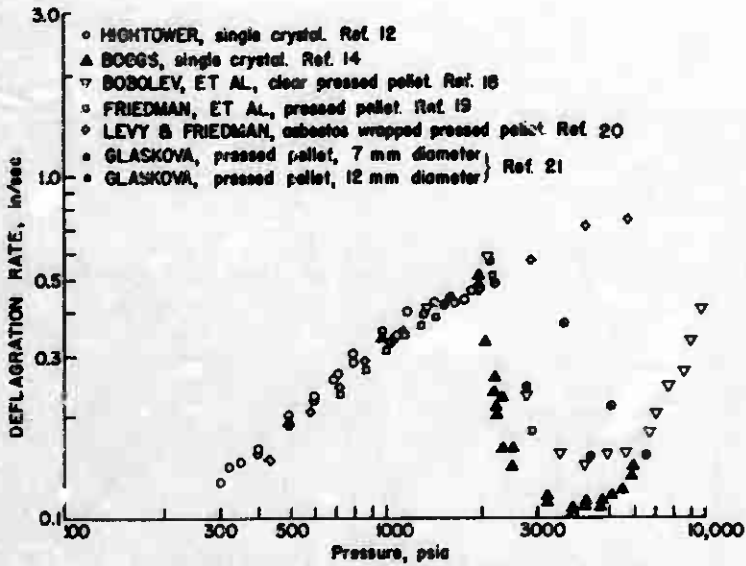
2. AMMONIUM PERCHLORATE DEFLAGRATION

When attention was directed to the structure of the combustion zone, it seemed appropriate to concentrate concurrently on the deflagration behavior of AP, since it is usually the dominant propellant ingredient. On burning and quenching single crystals of AP, it was quickly found that prevailing views regarding the deflagration were extremely naive. The burning surface exhibited certain reproducible irregularities, that were dependent on pressure (Ref. 4, 7, 12, 13 and 14). A previously unreported liquid layer was observed (Ref. 4, 5, 7, 12, 13 and 14), which appeared to encompass a significant portion of the rate-controlling reactions. Although such a layer is not embodied in any analytical models, its role seems to be crucial, and its presence resolves some earlier controversies regarding the rates and relative importance of solid, surface and gas phase reactions. During the present reporting period, these studies have been extended to higher pressures, and have revealed even more complicated behavior (Ref. 14). The investigations of the deflagration of single crystals were carried out to ascertain: (1) the variation of the deflagration rate as a function of pressure, (2) the surface structure of the deflagrating samples, and (3) the sub-surface profile associated with the deflagration. From these observations energy transfer modes were postulated.

Data concerning the variation of deflagration rate versus pressure from our investigations and those of other laboratories are compared in Fig. 2.1. Our results, obtained using cinemicrophotography, confirm the trend described by Bobolev, et al, and Glaskova. Some differences between their data and ours might be expected as they used pressed pellets and we used single crystals of AP.

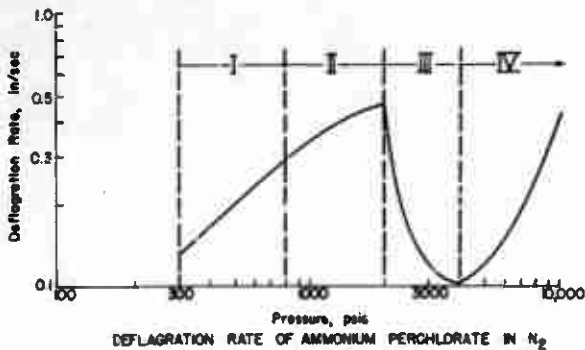
We observed that the single crystal data define a curve which naturally appears to be divided into four regimes (Fig. 2.2). Not only do these divisions apply to the deflagration rate curve but also to the results of the surface and subsurface structures of the deflagrating samples. The behavior is summarized in Table 2.1. The four regimes characterize the deflagration of AP crystals at pressures from 300 to 10,000 psia, thus permitting predictions of AP behavior during deflagration from a knowledge of the pressure.

Scanning electron microscope (SEM) micrographs taken of samples from Regime 1 indicate that the surface was covered with a froth: gas evolved through a liquid layer (Fig. 2.3). This observation permitted a choice to be made between two competing hypotheses. The widely



DEFLAGRATION RATE OF AMMONIUM PERCHLORATE IN N₂

FIG. 2.1. Deflagration Rate of Ammonium Perchlorate in Nitrogen Atmosphere.



DEFLAGRATION RATE OF AMMONIUM PERCHLORATE IN N₂

FIG. 2.2. Deflagration Rate of Ammonium Perchlorate Single Crystals in Nitrogen Atmosphere.



FIG. 2.3. Scanning Electron Micrographs of Ammonium Perchlorate Single Crystals Which Were Quenched While Undergoing Deflagration at the Pressures of Regime I.

accepted assumption that the mechanism of AP deflagration was the same as decomposition (i.e., sublimation) was not seriously questioned until Hightower (Ref. 4, 5, and 12) observed a cooled froth on the surface of quenched samples which he examined using an optical microscope. Scanning electron microscope analysis revealed the details of this froth and it was apparent that a melt had been present on the surface of the deflagrating sample. Such observations proved that the sublimation hypothesis was inaccurate to describe the deflagration. The froth on the AP crystal surface was shown to be roughly 1 to 5 microns thick on the 300 and 600 psia samples and present only in patches on samples burned at 800-900 psia. Examination of the profile showed that this froth, the thickness of which decreased with increased pressure, covered a layer of material which had been cubic phase AP, which in turn covered the original orthorhombic phase. The well defined interface between the cubic and orthorhombic phases indicates the location

Regime	Pressure, psi	Rate, in/min	Rate, as a Function of Press. Increase	Regression	Surface		Subsurface		Energy Transfer
					Characteristic	Function of Press. Increase	Characteristic	Function of Press. Increase	
I.	300-800	0.13-0.3	$r = cp^n$ where $n = 0.77$	Steady planar	Gee entrapped in liquid resulting in a froth	Thickness of liquid layer decreases, amount of gee increases	Froth in cubic phase, cubic phase on orthorhombic phase	Cubic phase thickness decreases, froth appears to decrease	"Exothermic" froth
II.	10 ⁴ -2000	0.34-0.48	Decreasing positive dr/dp	Steady macroscopically planar	Ridges & valleys with activity sites in valleys, surface pattern especially dependent with time	Length of ridges decreases, activity sites go from orthovigorous reaction sites & a few needles	Ridges & valleys composed of cubic phase, activity sites extend depth of cubic phase	Cubic layer under valley decreases, height between ridges & valleys increases	Condensed phase and gas-phase coupled
III.	2000-4000	0.48-0.10	Negative dr/dp	Intermittent nonplanar	Needles in areas of max. regression		Thickness of layer of needles = 200-300 u. no needles at areas of min. regression		Intermittent flame, localized decomposition in needle array
IV.	>4000	>0.10	Positive dr/dp	Steady macroscopically planar	Entirely covered by needles		Surface layer of needles on solid		Steady flame with uniform array of needles

Table 2.1

of the 242°C isotherm within the crystal. Knowledge of the position of this isotherm and the regression rate as a function of pressure allows a calculation of the surface temperature of deflagrating crystal (Ref. 15). Results obtained by using the SEM data were more precise than those Beckstead and Hightower obtained using the optical microscope, and were in agreement with the "best" line drawn through their data.

Samples from Regime II differed from those of Regime I in that no longer was there a liquid on the surface, rather the surface was characterized by a pattern of ridges and valleys (Fig. 2.4a) with sites of increased activity at the bottom of the valleys (Fig. 2.4b). Ridge length was found to vary inversely with the pressure (over 500 microns long at 1000 psia and less than 100 microns at 1800 psia). Just as the ridge structure was pressure dependent so were the sites of increased activity (reaction) at the bottom of the valleys. The samples quenched at 1000 psia show frothy residue in the valleys. The samples quenched at 1200 psia show frothy material, but also show holes of complex geometry indicative of localized activity. At 1500 psia an array of needle-like structures appeared in some of the holes. This feature becomes increasingly evident with increasing pressure.

The profiles of Regime II samples present evidence of the complex nature of the combustion. The cubic phase thickness was greater under the ridges than under the valleys (Fig. 2.4c). This difference in thickness indicates that the regression rate of the ridges was less than that of the valleys, that the temperature gradient through the ridges was not as steep as under the valleys, and that heat was transferred in three dimensions (including conduction of heat in direction perpendicular to the direction of the average surface regression). This interpretation would explain why the ridges frequently peeled off from the surface without burning, as seen in the high speed motion pictures. Figure 2.4d indicates that the activity sites of the valley extended below the surface for a depth almost equivalent to the cubic phase thickness.

The surfaces of the Regime III samples show pronounced depressions (Fig. 2.5) which have extensive areas of needles. The micrographs of the profiles indicate that the needles extend 200 to 300 microns from the surface of the pocket. Studies using cinemicrophotography identified the origin of these depressions and helped explain why the needles exist only in the depressions. These high speed motion pictures show localized orange flamelets, which change location as the burn progresses, over the surface. Parts of the surface were seen to regress locally (causing the depressions seen in the micrographs) while adjoining areas were temporarily stationary, with the flame standing over the recessed areas. Because the flame was observed to be in the depression, the lip seen in Fig. 2.5 provides an opportunity to view a portion of the sample which was partially exposed to the flame and at the same time view a

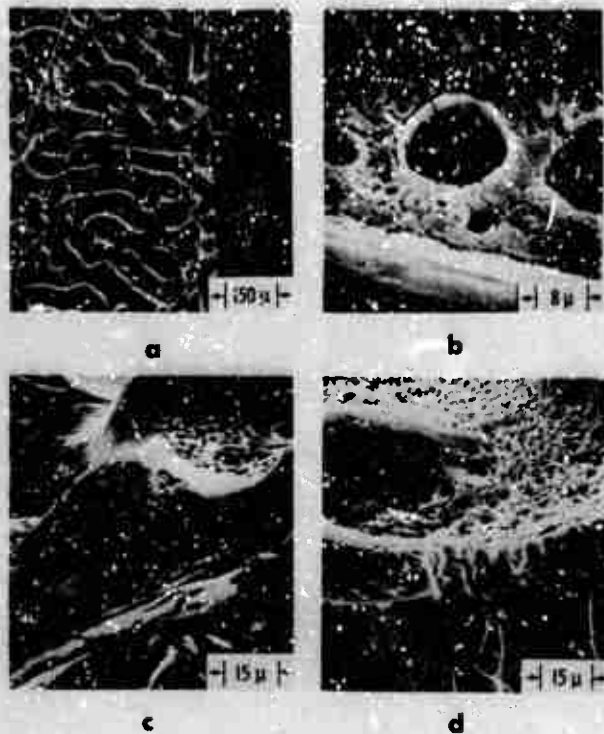


FIG. 2.4. Scanning Electron Micrographs of Ammonium Ferchlorate Single Crystals Which Were Quenched While Undergoing Deflagration at the Pressures of Regime II.

portion which was shielded from the flame. That portion which the flame contacted exhibits the needle structure, while the shielded portion exhibits a different surface structure. Thus by combining the SEM results with those obtained using cinemicrophotography it is possible to show that the needle structures are indicative of proximity to the flame. Scanning electron microscope micrographs taken of Regime IV samples show that needles covered the entire surface (Fig. 2.6) and the high speed motion pictures show a pronounced orange flame adjacent to the burning surface, thus confirming the above hypothesis.

From these observations we hypothesized as to how energy was transferred to the unreacted AP. At the low pressures of Regime I we have seen that the surface is covered with a froth. It is our hypothesis that decomposition occurs either within or beneath the melt and that

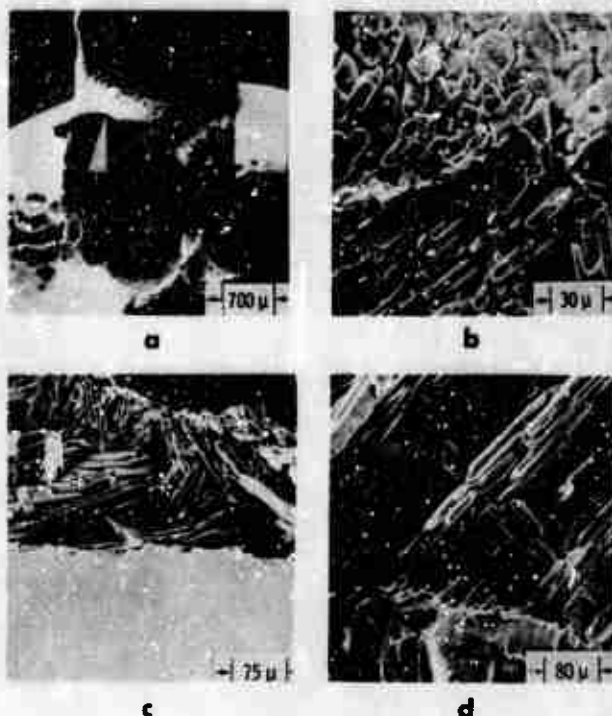


FIG. 2.5. Scanning Electron Micrographs of Ammonium Perchlorate Single Crystals Which Were Quenched While Undergoing Deflagration at the Pressures of Regime III.

exothermically reacting gaseous products are entrapped within the melt. The heat produced by the exothermic reaction is transferred by conduction through the froth to the unreacted solid, thereby providing the energy required for further decomposition. Further exothermic reaction probably occurs in the gas above the surface, although the heat transfer from those reactions may be secondary in importance. As the pressure is increased the liquid becomes so thin that it ruptures into droplets and the high reaction rate in these droplets is responsible for producing the valleys. The reactions become concentrated within the valleys and three-dimensional heating occurs within the solid.

While exothermic reactions within the froth and activity sites within the valleys are responsible for most of the energy transfer occurring in Regimes I and II, energy is primarily transferred to Regime III and IV samples by conduction from the gas flame. In Regime III the unsteady

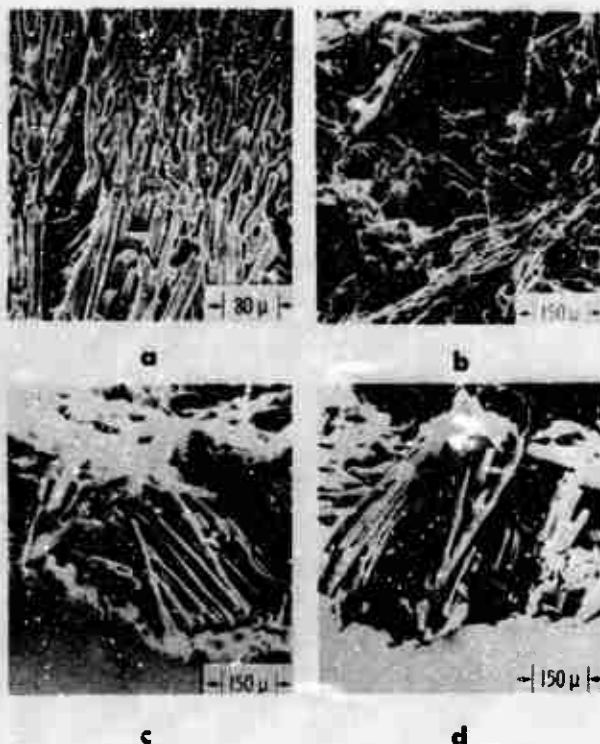


FIG. 2.6. Scanning Electron Micrographs of Ammonium Perchlorate Single Crystals Which Were Quenched While Undergoing Deflagration at the Pressures of Regime IV.

flame caused an areawise "atop and go" regression of the surface. In Regime IV the flame is steady and the deflagration rate once again increases.

A more complete description of the recent work under this program is contained in Ref. 6, 14, 16 and 17. From the results it is clear that AP deflagration is a very complex process, quite different from the assumptions of analytical models, and possibly amenable to modifications not previously suspected. It is interesting to note that most analytical models of composite solid propellant combustion rest on incorrect assumptions regarding AP deflagration, including AP deflagration rate curves that completely ignore the drop in burning rate above 2000 psi. Thus the propellant burning theories are gravely in error, even if they do (with adjustment of undetermined parameters) successfully correlate experimental results.

3. PROPELLANT COMBUSTION MECHANISM

The most conspicuous problem in combustion instability research has been the continuing ignorance of the nature of the combustion zone whose perturbations cause instability. During the present reporting period, several investigations were directed towards a better understanding of steady-state combustion and combustion zone structure.

3.1. ONE-DIMENSIONAL ANALYSIS OF COMBUSTION ZONE STRUCTURE

Most analytical models of steady-state burning of solid propellants can be referred to as "complete" in a mathematical sense, in that solutions are entirely a consequence of the set of equations in the model (with a few undetermined constants). Such models are both complex and naive. They are complex in that even simplified representations of the combustion zone behavior are analytically complicated. They are naive in that the simplified representations ignore important aspects of the real process (such as three-dimensionality, inhomogeneity of the propellant).

In attacking the problem of combustion zone structure, it appeared that one-dimensional models were really only computational schemes to aid physical insight, and as such should be formulated with a maximum flexibility to accommodate experimentally observable information such as combustion zone thickness and burning rate-pressure data. With this philosophy in mind, a one-dimensional model was constructed which was not "complete", and could accommodate input data on combustion zone location and thickness, burning rate, etc.

The model is an elementary one in which an assumed surface pyrolysis is followed by a gas phase reaction. The gas phase reaction rate is assumed to be constant in the reaction zone, which starts at some parametrically specified distance from the surface. The solution used here is sort of an inverse one in which all required thermodynamic, kinetic and transport properties are specified as well as the burning rate-pressure curve.

Calculations based on observed burning rate-pressure functions yield values for the heat release, flame thickness and stand-off distance required to give the specified burning rate. Using plausible values for thermodynamic, kinetic and transport properties, the results for flame thickness, etc., are well within the ranges observed. It appears then that this approach may be useful for examining the gross

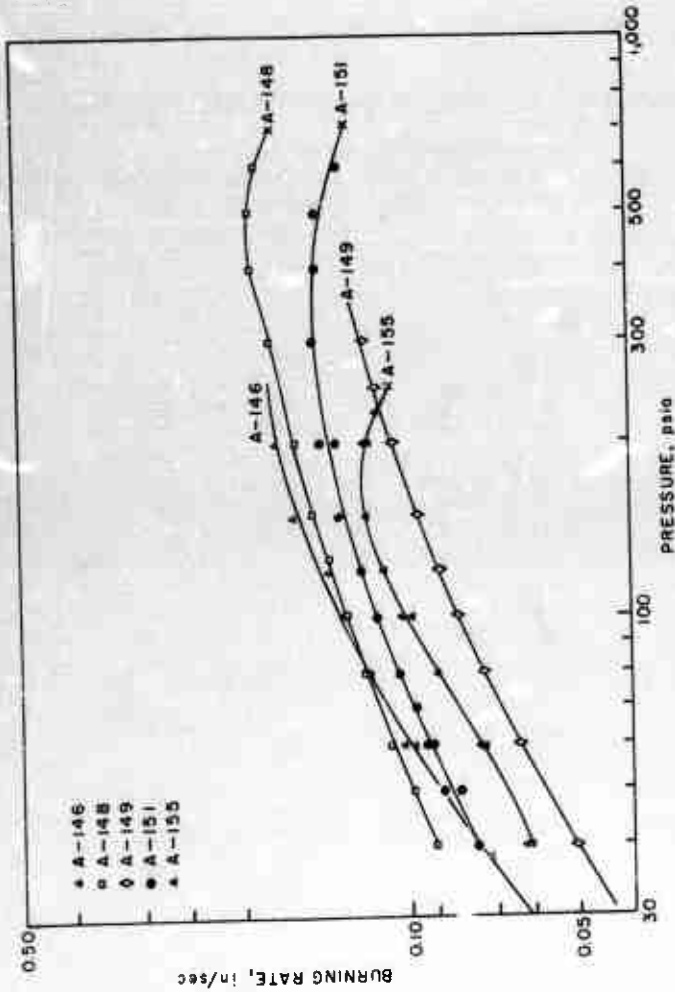


FIG. 3.1.1. Burning Rate Curves for Polyurethane-Ammonium Perchlorate Propellants.

effects of some of the parameters, such as surface activation energy, and thereby helping relate burning rates to chemical composition. The simplicity of the analysis enables one to perceive easily the physical origin of the results, a feature which is often not true in more sophisticated models. The results will be useful in studies of more complex models, be of value for examining limiting conditions for time dependent models, and be helpful in design of experiments to measure combustion zone structure. Further, the calculations will help to recognize the conditions under which one-dimensional models are useful, and conditions under which three-dimensional modeling is important.

Results to date are summarized in detail in Ref. 22 and 23.

3.2. BURNING RATE OF "BIMODAL" PROPELLANTS

It was observed in bulk mode instability tests that the trend of instability behavior was different for propellants made with bimodal oxidizer particle size distribution than for propellants with unimodal particle sizes. In correlating the test results, it is customary to use the steady-state burning rate as a normalizing variable in the frequency scale, and burning rate determinations were made accordingly. It was observed that the dependence of burning rate on pressure of unimodal propellants was quite different from the $\bar{r}(\bar{p})$ function for bimodal propellants. In hopes that understanding of the contrasting steady-state behavior might provide some clue to the contrasting perturbation behavior, a careful study of the burning rate was made of certain unimodal and bimodal formulations used in L^* burner tests.

The strand burning rates of two classes of propellants were determined as a function of pressure. One series of propellants consisted of polyurethane and bimodal AP (PU-AP) and the other consisted of carboxyl-terminated polybutadiene and bimodal AP (CTPB-AP). The formulations for the propellants are given in Table 3.1.

The data for the PU-AP propellants are presented in Fig. 3.1. The trend of higher burning rates for propellants having smaller oxidizer particles is apparent (compare the rates for A-146 versus those for A-149). Also it is seen that many of these propellants extinguish at high pressure: the approximate upper deflagration limit for 1/4- by 1/4-inch strands denoted by an x in the figure. The mechanism responsible for this extinguishment is discussed in Section 3.3. The mesa-burning rate and extinguishment characteristics of the PU-AP can be altered by inclusion of as little as 1% of a catalyst such as n-butyl ferrocene (Fig. 3.2).

The burning rate curves for the CTPB-AP propellants are presented in Fig. 3.3. These propellants do not exhibit the mesa characteristic nor the extinguishment seen for the PU-AP propellants. The SEM micrographs presented in Section 3.3 have shown that while the polyurethane binder melts, the CTPB binder gasifies without melting. It seems likely

TABLE 3.1. Composition of Research Propellants

Propellant designation	Ingredients and weight percent				
	Ammonium Perchlorate		Binder		Other
A-146	37.5%	15 μ	37.5%	80 μ	25% polyurethane
A-148	37.0%	15 μ	37.0%	200 μ	25% polyurethane 1% carbon black
A-149	37.0%	90 μ	37.0%	600 μ	25% polyurethane 1% carbon black
A-151	37.0%	45 μ	37.0%	200 μ	25% polyurethane 1% carbon black
A-155	37.0%	45 μ	37.0%	400 μ	25% polyurethane 1% carbon black
A-156	51.8%	15 μ	22.2%	200 μ	25% polyurethane 1% carbon black
A-157	22.2%	15 μ	51.8%	200 μ	25% polyurethane 1% carbon black
A-158	37.2%	90 μ	37.5%	600 μ	25% polyurethane
A-159	36.0%	15 μ	36.0%	200 μ	25% polyurethane 1% carbon black 1% n-butyl ferrocene
A-160	36.0%	45 μ	36.0%	400 μ	25% polyurethane 1% carbon black 1% n-butyl ferrocene
A-167	37.0%	15 μ	37.0%	80 μ	25% CTPB 1% carbon black
A-168	37.0%	15 μ	37.0%	200 μ	25% CTPB 1% carbon black
A-169	37.0%	90 μ	37.0%	600 μ	25% CTPB 1% carbon black
A-170	37.0%	45 μ	37.0%	200 μ	25% CTPB 1% carbon black
A-171	37.0%	45 μ	37.0%	400 μ	25% CTPB 1% carbon black
A-172	51.8%	15 μ	22.2%	200 μ	25% CTPB 1% carbon black

that the mass and extinguishment behavior of the PU-AP propellant is caused by an accumulation of molten binder on the surface.

A number of analytical models have been proposed for steady-state burning of solid propellants (Ref. 24-27, see also references cited in Ref. 25). Of these the best correlation with experimental data is provided by the granular diffusion flame (GDF) model proposed originally by Summerfield, et al (Ref. 27).

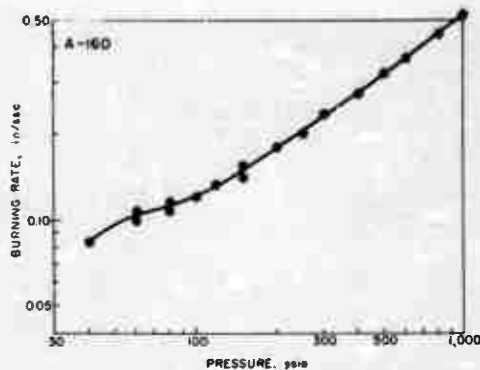


FIG. 3.2. Burning Rate Curve for a Polyurethane Ammonium Perchlorate Propellant Containing 1% n-butyl Ferrocene Catalyst.

The GDF model predicts that the burning rate will be related to pressure according to the expression $p/r = e + bp^{2/3}$. This expression predicts that plots of p/r versus $p^{2/3}$ will be straight lines, with a single value of the intercept a for a given chemical composition of propellant. The data of this study, when plotted in this manner, give the plots of Fig. 3.4 and 3.5.

As can be seen, the GDF model does not implicitly correlate either set of data, although it provides a rough fit to the CTPB data. The discrepancy between the CDF model and the PU-AP data is drastic and is presumably due in part to the role of the molten binder. The discrepancy in the case of the CTPB-AP data has qualitative importance and may be due to the bimodal oxidizer particle size distribution. Particle size distribution, an attribute of the propellant not embodied in existing models, is important when trying to predict the burning rates of in-service propellants which may have bimodal or trimodal AP particle size distributions. In both cases, the microscopic heterogeneity of the propellant appears to have a substantial effect on the burning rate characteristics, but is absent from published models.

In view of the complicated dependence of the burning rate on pressure observed in this study, the use of $r = cp^n$ or $p/r = a + bp^{2/3}$ for anything other than a first approximation is unwise. In particular, the use of $r = cp^n$ in the several perturbation models for solid propellant combustion instability must lead to some misrepresentation of the pressure dependence of the response function.

Further details on this work are available in Ref. 6.

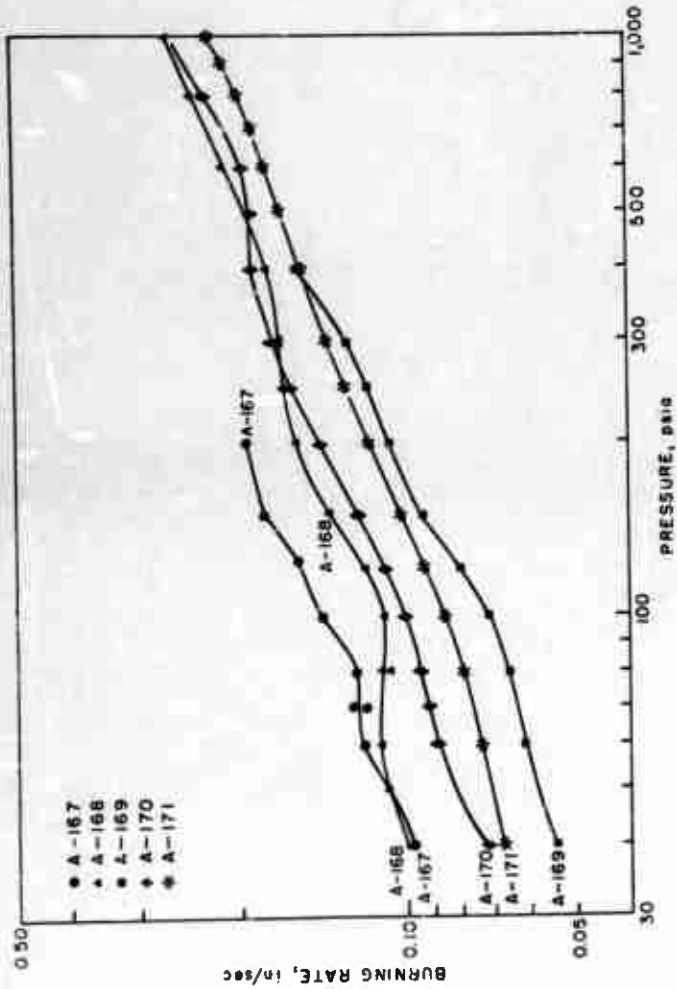


FIG. 3.3. Burning Rate Curves for Carboxyl-Terminated Polybutadiene-Ammonium Perchlorate Propellants.

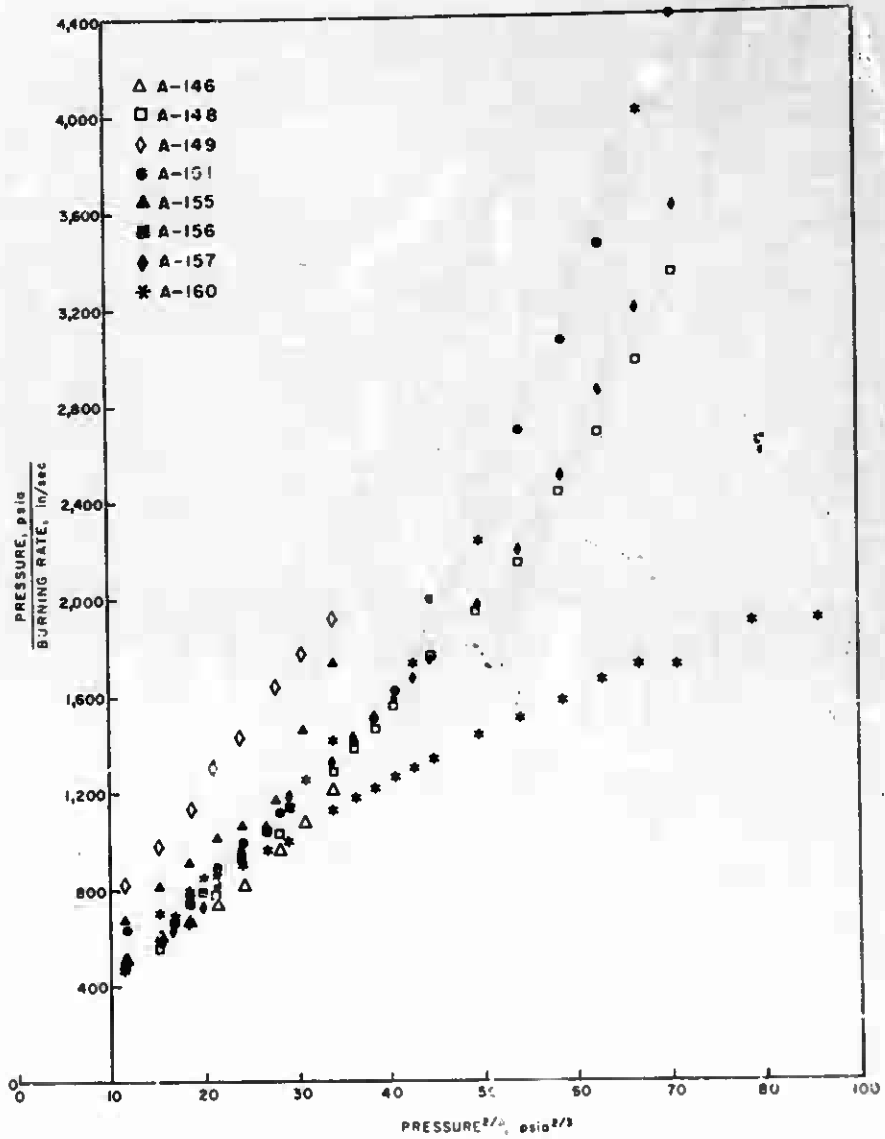


FIG. 3.4. Data for the Polyurethane-Ammonium Perchlorate Propellants Plotted in the Manner Suggested by the Granular Diffusion Flame Model Correlation.

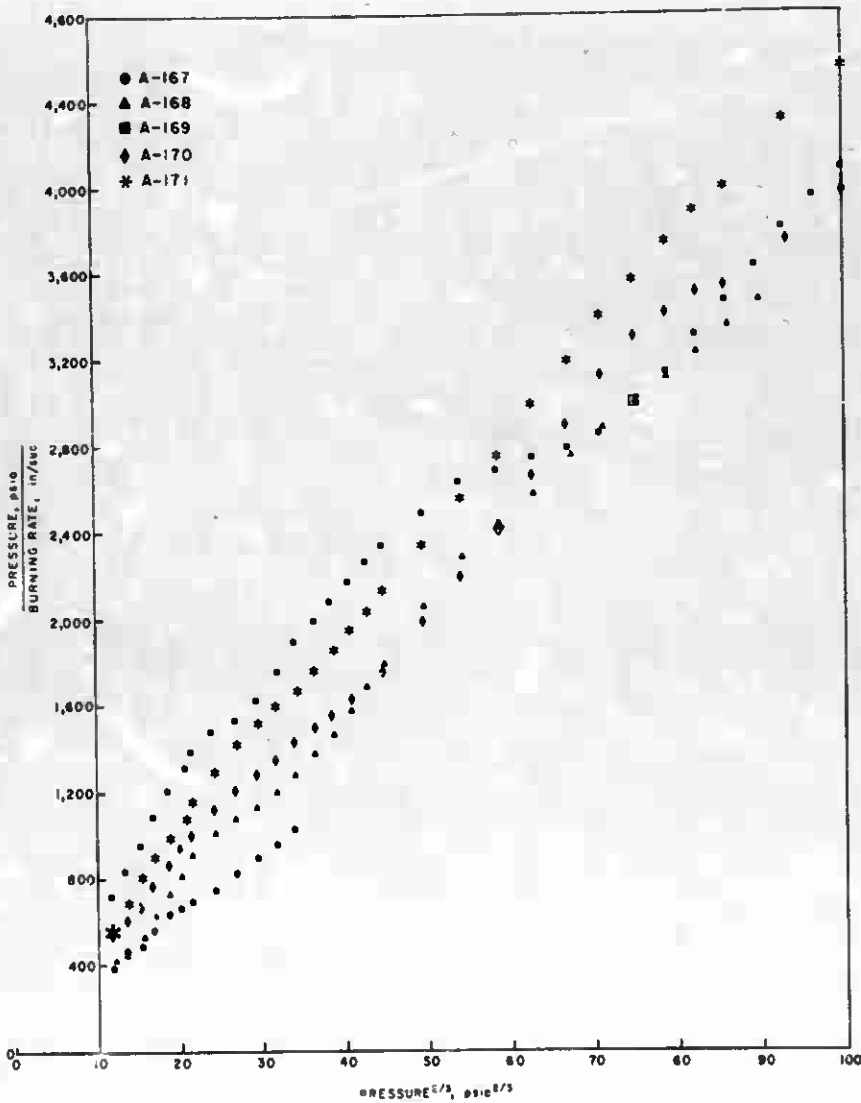


FIG. 3.5. Data for the Carboxyl-Terminated Polybutadiene-Ammonium Perchlorate Propellants plotted in the Manner Suggested by the Granular Diffusion Flame Model Correlation.

3.3. SURFACE STRUCTURE OF COMPOSITE SOLID PROPELLANTS

In order to quantitatively predict the combustion behavior of solid propellants it is necessary to reduce the description of this behavior to a set of relations which are amenable to mathematical expression. The surface structure of a burning solid propellant must be considered when attempting to mathematically model the propellant combustion. The majority of models proposed for steady and unsteady combustion of solid propellants treat the burning surface as a planar, dry, homogeneous entity with one simple Arrhenius expression describing the kinetics of the processes over the entire surface. For composite propellants, this obviously is not the case. One justification for such simplification is that the complex reality is approximated by a more tractable mathematical representation. Another reason is that detailed information defining the structure of the surface accurately enough to construct such a model is not available. Because of the latter reason, we initiated an experimental investigation to provide a better understanding of the physical nature of the surface and determine, if possible, the extent of heterogeneous or surface reactions. In this study burning propellant samples were quenched and then examined using an SEM to infer the structure of the burning surface prior to quench.

The unmetallized propellants tested consisted of a crystalline oxidizer and either polyurethane or carboxy-terminated polybutadiene (CTPB) binder. The propellants were formulated with either a unimodal oxidizer particle size distribution or a narrow-cut bimodal distribution, with no additives such as burning rate catalysts or powdered metal. Small strands of these propellants were burned at pressures between one atmosphere and 800 psia in a combustion bomb containing an inert gas. Once steady-state conditions were attained, the sample was extinguished by rapid depressurization of the combustion bomb. The extinguished samples were cut to an appropriate size, plated with a gold-palladium alloy of a few angstroms thickness, and examined and photographed by using the SEM.

Results typical of this study are shown in Fig. 3.6-3.10. Figure 3.6 presents SEM micrographs of samples consisting of AP and a polyurethane binder which were burned at pressures of 100 psia (Fig. 3.6a-b) and 200 psia (Fig. 3.6c-f). Inspection of the photographs reveals that at low pressures the pyrolysis rate of AP was less than that of the polyurethane binder, thus confirming the observation reported by Baatres (Ref. 24) that the AP protrudes above the binder at low pressures. Also, the smooth appearance of the binder suggests that it was molten during burning. It is of interest to note that all of the views shown in Fig. 3.6 (PU-AP propellant) indicate definite undercutting of the binder-oxidizer particle boundary. Such undercutting illustrates the error of using one space coordinate to try to describe the combustion. Figure 3.7 illustrates the effects of pressure on the surface structure. The photographs on the left (Fig. 3.7a, c and e) are of samples obtained at



FIG. 3.6. Scanning Electron Microscope Micrographs of Polyurethane-Ammonium Perchlorate Propellant Which was Quenched While Burning at 100 psia (a-b) and 200 psia (c-f).

100 psia while those samples on the right (Fig. 3.7b, d and f) were obtained at 800 psia. Both sets of samples conclusively demonstrate that the binder was molten prior to quench. At the lower pressure the AP crystals protrude above the binder surface and undercutting is again noted. At the higher pressure, the crystals are recessed below the binder surface to the extent that the molten binder has apparently flowed into the recesses and covered the crystal surfaces (possibly during extinguishment). This phenomenon provides an explanation of why some

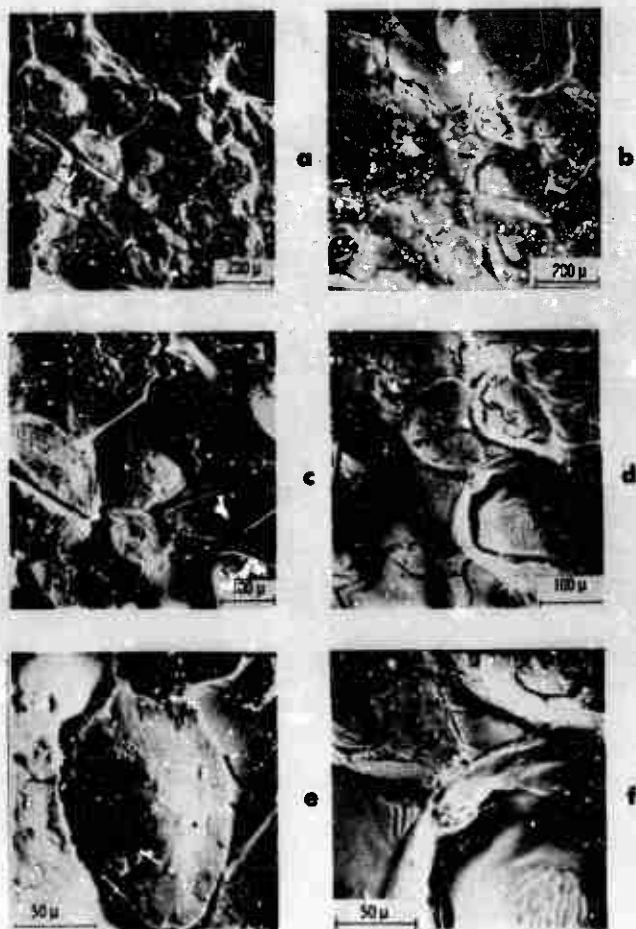


FIG. 3.7. Scanning Electron Microscope Micrographs of Polyurethane-Ammonium Perchlorate Propellant which was Quenched While Burning at 100 psia (a, c and e) and 800 psia (b, d and f).

polyurethane propellants do not sustain combustion at pressures above approximately 600 psia as previously reported (Ref. 28). As the pressure is increased the regression rate of the AP eventually becomes greater than the binder regression and the molten binder then flows over the AP crystals inhibiting their combustion and causing extinguishment.

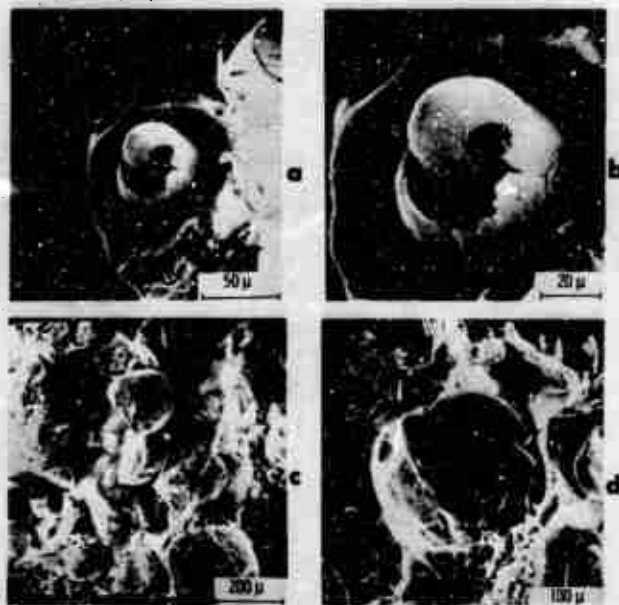


FIG. 3.8. Scanning Electron Microscope Micrographs of Polyurethane-Ammonium Perchlorate Propellant Which was Quenched While Burning at 100 psia.

Earlier we showed that, under certain conditions, AP crystals have a surface melt. Prior to the SEM studies described here, there had been considerable controversy surrounding the question of whether these crystals in the propellant matrix melted or sublimed during combustion. The SEM permitted us to make a detailed examination of quenched propellant samples which showed that the AP in a burning propellant was molten (Fig. 3.8 and 3.9). The bubble formation shown in Fig. 3.8 is typical of the structure seen on quenched samples of AP which was interpreted as evidence that the surface of the AP consists of a thin molten layer during burning. Gases formed from the decomposition of the crystals within the molten layer expanded during rapid depressurization causing the bubble formation as the melt froze. Indeed it would be difficult to explain the bubble-like structure without assuming the existence of a liquid state. Similar types of structures are evident in Fig. 3.6 and 3.9 as well as in the majority of the samples studied. The volcano-like structure seen in Fig. 3.6a, e and f and Fig. 3.9, and the vented structure shown in Fig. 3.6c-d also indicate that subsurface reactions have taken place within the crystal prior to quench. These structures are in agreement with those observed when pure single crystals of AP are burned, quenched, and examined.

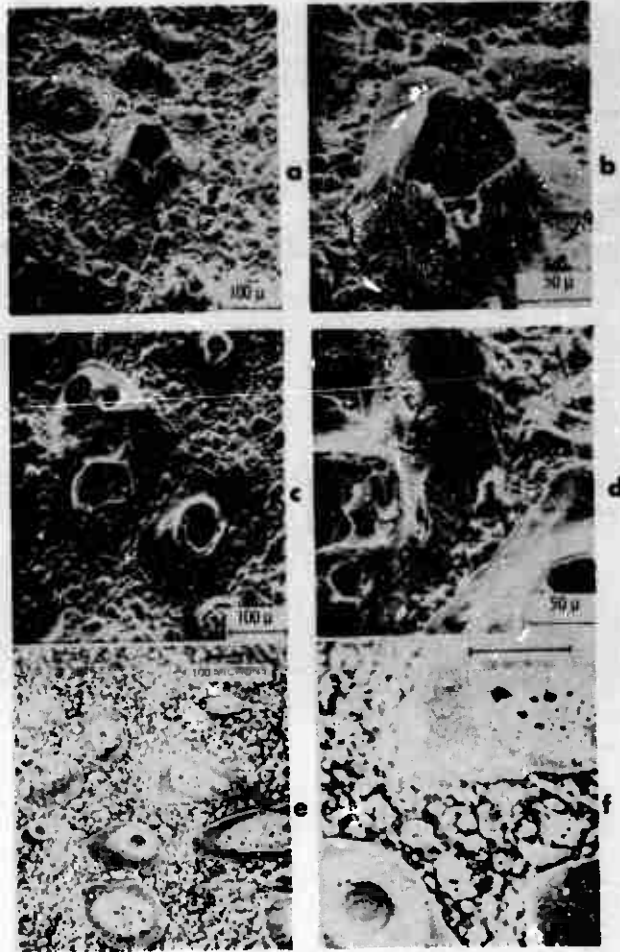


FIG. 3.9. Scanning Electron Microscope Micrographs of Carboxyl Terminated Polybutadiene-Ammonium Perchlorate Propellant Which was Quenched While Burning at 600 psia.

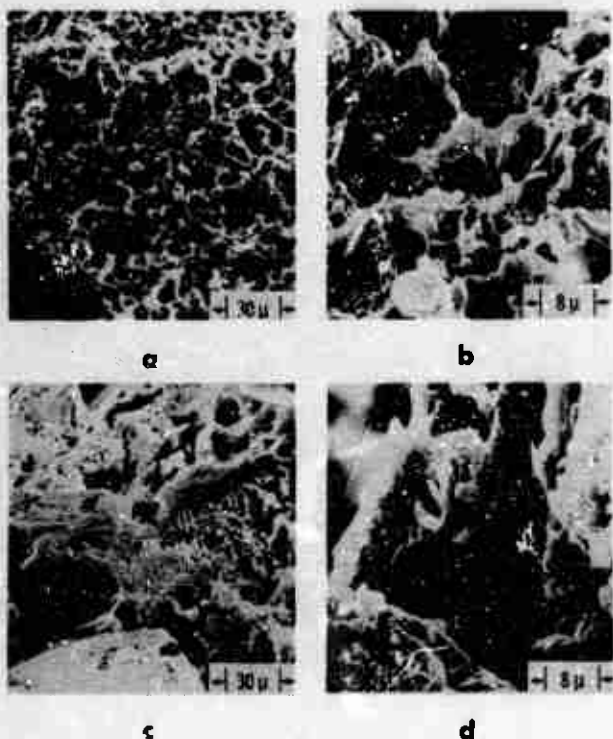


FIG. 3.10. Scanning Electron Microscope Micrograph of an HMX-Polyurethane Propellant.

By mechanically stressing the quenched samples it was possible to break the AP-binder bond, releasing the crystals as seen in Fig. 3.8. Examination of the displaced crystals shown in Fig. 3.8c and one of the crystals left undisturbed in the binder as seen in Fig. 3.8d shows no indication of subsurface or interfacial reaction between the AP and the binder.

In order to explore the effect of binder-type on the surface structure, a propellant containing a carboxy-terminated polybutadiene (CTPB) binder was tested. Results from these tests at 600 psia are included in Fig. 3.9. The micrographs indicate that the surface of the AP crystals was molten and that subsurface reactions in the molten phase of the AP resulted in gas liberation within the molten phase. The micrograph seen in Fig. 3.9d and f seems to indicate that interfacial reactions were not present at the binder-oxidizer (CTPB-AP) interface at this pressure. No

undermining was observed on samples obtained at other pressures, indicating a lack of interfacial reactions with the CTPB samples. Also, there is no indication of the CTPB binder melting as with the polyurethane binder (i.e., the binder does not have a smooth appearance nor the "cracked-mud" appearance of Fig. 3.7).

Study of the behavior of oxidizers other than AP in the combustion zone has been rather limited. However the various crystalline oxidizers of interest differ widely in their high temperature behavior, and an objective view of combustion zone processes cannot be formulated on the basis of AP propellants alone. Figure 3.10 shows SEM pictures of the quenched surface of a propellant with a polyurethane binder and HMX (cyclotetramethylenetetranitramine). The melting point of HMX is so low (280°C) that it would be molten to an appreciable depth beneath the propellant surface. From examination of Fig. 3.10 it is evident that the HMX was decomposing at an appreciable depth below the surface, with a very "turbulent" surface (Fig. 3.10a-b) and bubbles to considerable depth (in cross-sections of the sample, Fig. 3.10c-d).

These investigations of surface structure of the combustion zone are continuing, including cooperation with an Air Force program at the Lockheed Propulsion Co. Further details of the work may be obtained from Ref. 16, and 29-31.

3.4. METAL AGGLOMERATION

The utility of including metallic fuels in propellants depends upon how efficiently the metal ignites, burns, and produces high temperature working gases. Aluminum as a fuel is being studied in detail because it is in widespread use, it frequently exhibits poor combustion efficiency and it is an important factor in driving axial mode and low frequency combustion instability. The current work is an investigation of the preignition behavior of aluminum, using a hot stage microscope, a gas laser, and the agglomeration, ignition, and combustion of aluminum on and near the surface of composite propellants.

3.4.1. Particle Preignition Studies

The experimental setup for the preignition studies of aluminum particles is described in Ref. 32. Two heating methods have been applied, namely heating on a microscope hot stage and heating by laser radiation. The first method produces only low heating rates ($\leq 900^\circ\text{C}/\text{min}$) but the temperature can be readily measured whereas the laser heating yields higher heating rates but makes temperature measurements very difficult or even impossible. After heating and cooling, the samples were examined with the optical microscope as well as the SEM. The results are presented in detail in Ref. 34 and will be described here only briefly.

Heating of spherical aluminum particula (105-125 μ diameter) in air at the relatively low rate of about 900 $^{\circ}$ C/min produced surface oxidation; in the areas where particles were touching, agglomeration at temperatures as low as the melting point of aluminum ($T_m = 659.7^{\circ}$ C) occurred. At a constant heating rate the amount of oxidation is a function of temperature, as shown in Fig. 3.11. Figure 3.11a shows the smooth but wrinkled surface of two agglomerated particula after heating to 690 $^{\circ}$ C. Heating to 845 $^{\circ}$ C did not change the smoothness of the oxide skin but resulted in severe cracking and wrinkling. This can be seen in Fig. 3.11b of a "bridge" connecting two agglomerated particles. In both cases wrinkling was observed to occur during cooling of the particles and hence is not of great concern to the preignition behavior. At 1040 $^{\circ}$ C the particles were oxidized to the extent that the resulting oxide shells were rigid and no longer could wrinkle on cooling. Consequently, the particles retained their spherical shape and exhibited a coarse granular structure of oxide surface (Fig. 3.11c). Some large spherical agglomerates were obtained. The spherical shape indicated that solid oxide (melting point $T_m = 2042^{\circ}$ C) was incorporated in the agglomerates. Finally, heating to 1200 $^{\circ}$ C increased oxidation to the point where the oxide on the agglomerate surface was granular (Fig. 3.11d) and much coarser than that obtained at 1040 $^{\circ}$ C.

Laser heating of spherical aluminum particles in air at high rates to temperatures below the melting point of aluminum oxide ($T < 2042^{\circ}$ C) resulted in heavy oxidation and agglomeration (Fig. 3.12a) very similar to that obtained on the hot stage microscope. Laser heating to temperatures above the melting point of aluminum oxide ($T > 2042^{\circ}$ C) led to fast oxidation of the individual metal particles with greatly reduced agglomeration (Fig. 3.12b). Heavy smoke indicated the transition to burning.

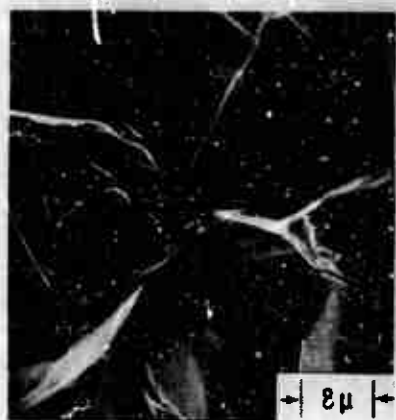
In summary, agglomeration on the hot stage occurred at rather low temperatures when oxidation was still at low level and the particles were in physical contact. Below 845 $^{\circ}$ C little oxidation occurred which favored agglomeration in that temperature range. Heavy oxidation made the oxide shells rigid and reduced agglomeration at high temperatures. Heating rate (by laser radiation) above the melting point of aluminum oxide favored the oxidation of the individual aluminum particle. No large agglomerates involving the flow of melted aluminum were observed. Instead, the oxide seemed to fuse together forming an irregularly shaped structure.

3.4.2. Aluminum Behavior in Propellants

In preceding reports a qualitative description of aluminum accumulation on the surface of burning propellants (referred to as the "pocket model") (Ref. 4) and the qualitative description of the microscopic details of the agglomeration processes (Ref. 5) were presented. Subsequent work in this area has been intermittent due to reduced funding;



(a)



(b)



(c)



(d)

FIG. 3.11. Aluminum Particles After Heating in Air to (a) 690°C, (b) 845°C, (c) 1046°C, and (d) 1200°C.



FIG. 3.12. Aluminum Particles After Heating in Air by a Laser Beam to Temperatures, (a) Below and (b) Above Melting Point of Aluminum Oxide.

it has been aimed at (1) obtaining more conclusive microscopic evidence of the aluminum sintering process, (2) measurement of aluminum agglomerate sizes from high speed, magnified motion pictures to provide a more quantitative basis for the "pocket model", and (3) combining all past work into a comprehensive open literature publication.

Earlier attempts to obtain partially burned samples of propellant for microscopic examination of the aluminum agglomerates (Ref. 5 and 33) by rapid depressurization and by thermal quenching on a stainless steel plate resulted in samples which did not show the details of the sintering process as conclusively as desired. Subsequently, samples of sinterized propellants were burned and thermally quenched using a copper vice heat sink (Ref. 7). Scanning electron microscope pictures of the samples quenched in this way are shown in Fig. 3.13 and 3.14; for comparison, Fig. 3.15 shows SEM photographs of 100 micron aluminum balls sintered together by impingement on a sapphire plate heated to 1400°C (Ref. 5).

Figure 3.13 shows successively magnified pictures from the SEM of one area of the burning surface of thermally quenched A-49 propellant which contained 16% 15 micron aluminum, 59% 200 micron AP, and 25% polyurethane binder. An AP particle approximately one-half consumed is evident in the upper center of Fig. 3.13a; the accumulation on top of the partially consumed AP is aluminum particles of approximately 15 micron diameter that are probably sintered together. The accumulation as a whole appears to be held onto the

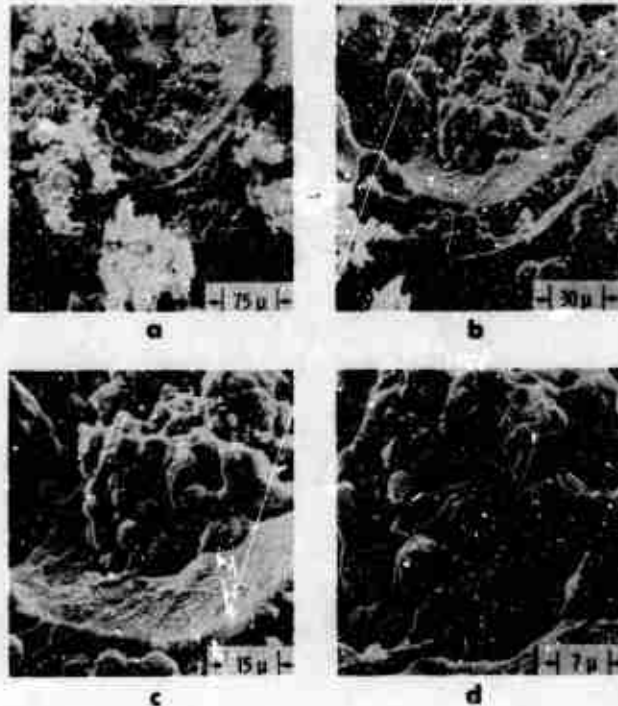


FIG. 3.13. Surface of Thermally Quenched Propellant Showing Accumulation of Aluminum of the Surface of the AP Particles and Binder.

surface of the AP particle by being wetted by the liquid AP surface (Ref. 13). In Fig. 3.13b sintered aluminum particula can be seen on the binder surface (in the foreground of the AP particle); these particula also appear to be held on the binder surface by being wetted by a liquid binder surface. Thus, these pictures are rather conclusive evidence that a major portion of the aluminum is retained on the surface of the propellant, either on the "wet" binder or "wet" AP surface. It appears that a very important factor in the agglomeration process is that during the time between the emergence of an aluminum particle on the surface and its inclusion as part of an agglomerate, it is held on the surface by this "wetted" condition. As the surface continues to recede, the population of the accumulated aluminum increases until the particles are in contact with one another. During this accumulation time, oxidative self-heating and increased proximity to the gas phase heat source raise the temperature of the aluminum to its melting point; at the melting point of aluminum, the sintering or "bridging" of the aluminum particula begins (Ref. 5).

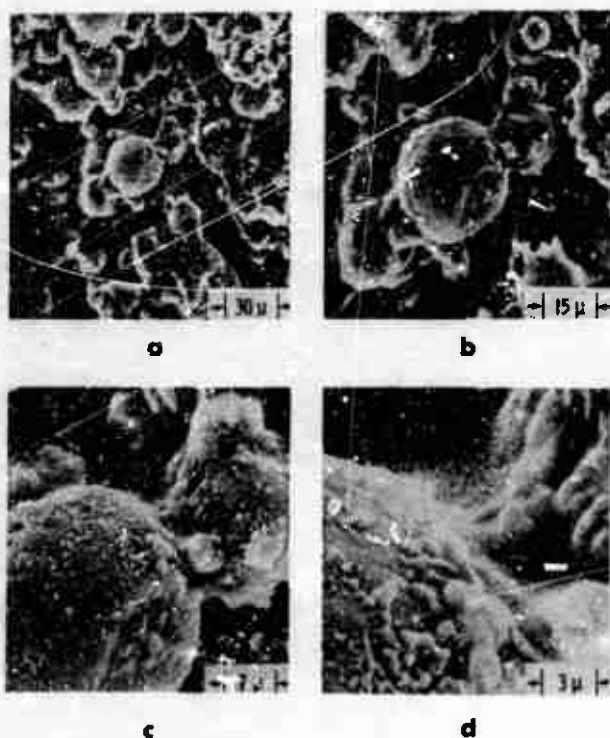


FIG. 3.14. Aluminum Agglomeration on Surface of Propellant Showing the "Bridging" Together of Particles.

Figure 3.14 shows SEM photographs of a thermally quenched sample of A-107 propellant which contained 16% 15 micron aluminum and 59% 600 micron AP. An assemblage of loosely sintered aluminum particles is shown in Fig. 3.14a. Successive magnifications are focused on the "bridge" of aluminum and/or aluminum oxide connecting two aluminum particles. This series of pictures when compared to those in Fig. 3.15 show the geometrical similarity between the "bridging" process on the surface of burning propellants and the more easily interpreted "bridging" process occurring during the rapid heating of 100 micron aluminum spheres in air (Ref. 5). Thus, the pictures in Fig. 3.14 are rather conclusive evidence that the sintering process that leads to formation of aluminum agglomerates in burning propellants is very closely related to the mechanistic description of the aluminum "bridging" process described in Ref. 5.

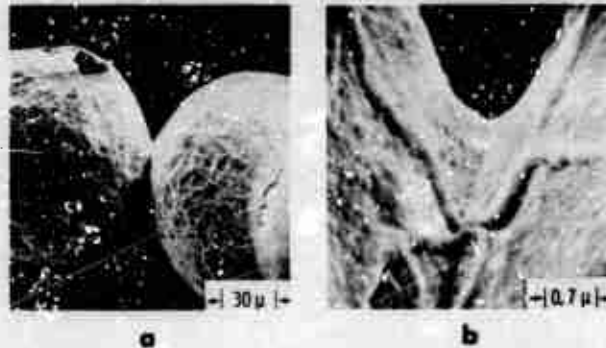


FIG. 3.15. Aluminum "Bridging of Heated Single Particles (Ref. 5).

During the course of organizing the material on aluminum agglomeration for an open literature publication, it became obvious that detailed measurement of the agglomerate size distributions was very desirable. Therefore, motion picture sequences from 18 tests of 14 different propellant formulations were selected for measurement. Most of the films have been measured and although there appears to be some discrepancies in the data, it appears that the quantitative information from the measurements is, in general, consistent with the qualitative picture of the "pocket model".

The procedure for determining the size-number distribution from the movie film was to count each agglomerate and measure its apparent diameter in a selected volume at some arbitrary time and to continue to count and measure the additional incoming agglomerates in subsequent consecutive frames until a minimum of 200 agglomerates had been measured. The volume selected for measurement was 4000 microns wide (slightly narrower than the film image width), 1500 microns thick (the thickness of the original propellant sample), and 1000 microns above the burning surface. The apparent agglomerate diameter was recorded in 10 micron increments. Representative data are presented in Fig. 3.16 where the ordinate, N' , of the histogram is the number of agglomerates normalized by the count of the most numerous size.

Since the "pocket model" states that the size of aluminum agglomerate is principally determined by the total volume of aluminum contained in the binder pocket between the AP particles and since the behavior of the total mass of aluminum is the quantity of interest, it is necessary to convert the number-diameter relationship to a relationship between the mass of the agglomerate and the size distribution. The data in Fig. 3.16 were converted to reflect the role of the mass of the agglomerates as shown in Fig. 3.17. In this figure, M' is the normalized total

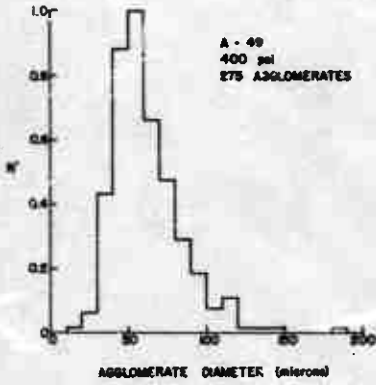


FIG. 3.16. Representative Number Distribution of Agglomerates Obtained From Movie Film

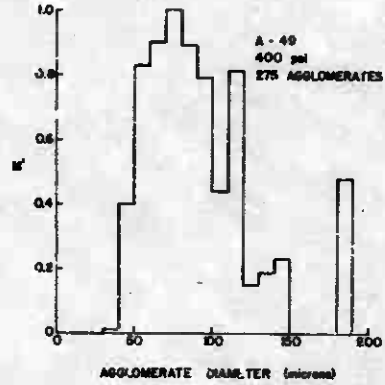


FIG. 3.17. Representative Mass Distribution of Agglomerates.

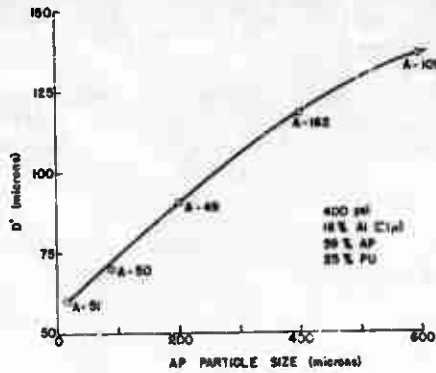


FIG. 3.18. The Effect of Changing the AP Particle Size on the "Mass Average" Agglomerate Diameter.

mass of the aluminum agglomerate; it was obtained by multiplying the normalized number of agglomerates, N' , by the cube of the appropriate diameter and normalizing with respect to the largest mass. In order to examine what effect a particular propellant variable had on aluminum agglomeration, it was necessary to represent the agglomerate mass distribution by a single number. The agglomerate diameter corresponding to the average normalized mass of all the agglomerates, i.e., the centroid with respect to the diameter of the M' versus agglomerate diameter histogram, was chosen as the variable for describing the agglomerate mass. Work is in progress on reducing the data to the form of "mass average diameter" as a function of propellant parameters.

An example of the type of information being obtained is shown in Fig. 3.18 where the "mass average diameter", d' , is plotted against the AP particle size. The trend of increasing agglomerate size with increasing AP size is in agreement with the pocket model. Similar data is being obtained as a function of original aluminum particle size, percentage of aluminum, pressure, binder percentage and binder type.

A paper for the open literature covering all the work on aluminum behavior is being prepared; its completion date is contingent on the completion and reconciliation of the reduced data.

3.4.3. Interpretation of Results

The results obtained by the various investigations provide a qualitative understanding of how and why aluminum accumulates and agglomerates in the combustion zone. Since aluminum is a pure element with a high boiling point, it does not decompose and/or gasify at the propellant surface temperatures ($\sim 600^\circ\text{C}$). It comes to the surface with a highly protective coating of oxide, and is surrounded by a flow of fuel vapors from the binder. Conditions are not particularly favorable for oxidation, although it may be appreciable when the aluminum is present in very fine particle size (e.g., $< 5 \mu$). Since the aluminum is seen to accumulate on the surface, there is apparently enough surface force to retain emerging particles (one would expect this to be dependent on the type of binder).

As the aluminum particles accumulate on the surface, they rise further in temperature due to protrusion towards the diffusion flame, and they crowd together as more particles emerge from the receding binder. From studies described above, it seems clear that the particles will "sinter" together when the aluminum melting point is reached, this process taking place by oxidation of aluminum leaking through the expansion cracks in the oxide shell. This leads to an irregular array of loosely held aluminum on the surface, which may continue to oxidize as the proximity to the diffusion flame increases and the oxide continues to crack due to difference in expansion coefficient of Al and Al_2O_3 . From motion pictures and quenched samples, it is clear that the metal resides for an appreciable time on the surface without inflammation. The material

is not mobile in this phase of the agglomeration. The increasing obstruction of gas flow by the growing agglomerate eventually provides forces sufficient for detachment from the surface. This trend is accompanied by chemical changes in the underlying material and surrounding gas flow, due to consumption of binder filaments and oxidizer particles. It would be difficult to know to what extent separation from the surface is due to increasing obstruction of flow, and to what extent due to changing surface forces and chemical environment. It seems likely that the consumption of a volume element of binder between oxidizer particles will leave an accumulate that consists of most of the metal from that fuel pocket. The emergence of an underlying oxidizer particle provides a transition in both fluid dynamic and chemical environment conducive to inflammation. This has led to the "pocket" model mechanism for metal agglomeration, and the results of the present studies on propellants with unimodal oxidizer particle size distribution (which led to the "pocket" model) indicate that the foregoing microstructure-related argument for agglomeration is relevant. However, results with propellants having polymodal oxidizer particle size (and no real "pockets") show agglomeration to the same range of droplet sizes, so that other factors such as protrusion of agglomerates into the diffusion flame can also be important factors in the agglomeration sequence. Further, at low pressures the agglomeration can be much more extensive because of the less favorable conditions for inflammation, and agglomerate droplets may result from inflammation of fairly extensive sintered layers of aluminum. This process is particularly conspicuous in "propellants" made by pressing powdered AP and aluminum without binder. Pellets made in this way exhibit massive agglomeration of aluminum, with the sintered layer being consumed intermittently by spread of inflammation from local initiation sites.

In most situations the agglomerate is seen to ignite in the process of leaving the surface, so that inflammation and separation constitute one complicated event. The sintered accumulate is seen to draw (or roll) up into a burning agglomerate droplet, which usually then leaves the surface (window bomb tests), but in some situations instead rolls around picking up more accumulate. Under some conditions particularly unfavorable to aluminum combustion, the agglomerate does not become fully inflamed, but instead remains a luminous, irregular agglomerate which hangs tenuously to the surface and eventually floats away without becoming a droplet.

Inflammation is an easily distinguishable event in most situations, because it involves the transition from a slowly rescaling, solid oxide-coated agglomerate to a rapidly rescaling droplet in which the oxide has melted and partly retracted from much of the aluminum surface. This stage is easily visible because the agglomerate becomes apherical, extremely luminous, has a visible oxide smoke trail, and the surface is clearly comprised of areas of oxide (high emissivity) and metal (low emissivity, with reflected highlights under external illumination). These observations are similar to those made in independent studies of

combustion of single aluminum particles in controlled atmospheric experiments (Ref. 32, 34 and 35) where oxygen is the principal oxidizing species.

The mobility of the agglomerate increases during or after inflammation: in the flow field of the rocket motor the droplet probably leaves the surface at this point, but in window bomb tests it sometimes wanders over the surface with further agglomeration. From the standpoint of overall combustion behavior, this point is probably quite important. Further agglomeration can affect efficiency of combustion of the metal in the motor. Retention of burning metal over the surface probably affects the burning rate of the propellant (in a pressure-dependent way). Susceptibility of this loosely held agglomerate to premature inflammation and/or separation from the surface by a flow disturbance may cause unstable burning. All of these factors are no doubt highly dependent on such variables as metal particle size, oxidizer particle size, stoichiometry, binder melting and decomposition characteristics, and gas flow environment. Because of the large number of variables involved, the continuing ignorance of binder and oxidizer pyrolysis, and the limited knowledge of the diffusion flame structure, the contribution of the metal to the various aspects of propellant combustion remains obscure. However, increasing qualitative understanding holds promise for rational ordering of experimental observations and for development of techniques to control metal combustion behavior.

4. BULK MODE INSTABILITY

Oscillatory combustion in low frequency, non-wave modes is a problem confined primarily to motors operating at low combustor L^* , typical of space motors and thrust magnitude control motors operating in low thrust mode. Analytical and laboratory testing of this phenomenon has been relatively successful because it is simpler than wave mode instability. A number of papers have been published recently on this problem, and recent work on this program is summarized in some of these references (Ref. 36-38), and will not be repeated here. Instead, a diagnosis of the state of knowledge and future needs is presented. This diagnosis emerged from a critical review of work of all agencies to date, a review that was stimulated by a judgement that the experimental results were telling the scientific community much more than we were hearing, and that our thinking was unduly inhibited by reliance on overly simplified analytical models.

4.1. STATUS OF KNOWLEDGE

Analysis of BMI consists of an application of conservation laws to the mass and energy transport in the combustor. Modeling of the combustion zone itself (usually assumed to be localized at the propellant surface) is the object of an additional collection of studies (Ref. 4 and 39) and may be incorporated into the combustor analysis by use of the "response function" concept, which represents the combustion zone in terms of its acoustic response, i.e., amplitude and phase of the burning rate oscillation produced by a given pressure oscillation. Linear analyses of mass conservation in the combustor lead to various forms (Ref. 36 and 40-45) of the equations

$$R \cos \omega t - \Gamma = \phi (\alpha L^*/c^*) \quad (4.1)$$

$$R \sin \omega t = \phi (\omega L^*/c^*) \quad (4.2)$$

where α and ω are the growth rate and frequency of the pressure oscillations; L^* describes the burner geometry (free volume/throat area); R and ωt are the magnitude and phase of the combustion oscillations; c^* is the usual effective discharge velocity of the nozzle; and Γ and ϕ have values near one, and are functions of the ratio of specific heats (exact values slightly sensitive to ratio of combustor flushing time to period of oscillation). The qualitative validity of these equations is apparently

not suspect, except when the volume of the combustion zone is comparable to the combustor volume (e.g., with metallized propellants at low combustor pressure). Application of the equations is of course dependent on knowledge of R and τ as functions of ω and other relevant variables.

Perhaps the largest source of uncertainty in BMI analyses is the limited knowledge of the response function and the qualitative sensitivity of the solutions of Eq. 4.1 and 4.2 to this range of uncertainty of R and τ . The qualitative dependence of R and τ on frequency is seen in both theory and experiment to be of the form shown in Fig. 4.1a. The corresponding solutions to Eq. 4.1 and 4.2 are shown in Fig. 4.1b. The calculations using Eq. 4.1 and 4.2 may proceed in either direction from Fig. 4.1a to 4.1b or from 4.1b to 4.1a, according to the needs of the situation (Ref. 36). (In the example, the curves in Fig. 4.1b were proposed first on the basis of a speculative interpretation of certain experimental measurements of α , ω and L^* mentioned later, and the form of the corresponding calculated response functions was used as a test of the plausibility of the postulated α - L^* curves.) The results suggest that the form of the solution α versus L^* differs qualitatively for rather modest changes in the response function.

Past studies of BMI have represented the response function in terms of one of the "QSHOD" analytical models for combustion perturbations (quasi-steady, gas phase, homogeneous propellant, one-dimensional models) (Ref. 39 and 46). These models have been used in papers on BMI primarily to analyze the stability trends defined by the $\alpha = 0$ condition. But they can be used also to develop a complete solution such as the normalized α versus L^* functions illustrated in Fig. 4.2. These functions were calculated from Eq. 4.1 and 4.2, the definitions of A and L^* indicated in the figure, and Eq. 17 and 43 of Ref. 39 (the quantities A and B are regarded in the QSHOD models as properties of the propellant, relatively insensitive to pressure or frequency, see Ref. 39). From Fig. 4.2 it is evident that considerable variation in the form of the α - L^* function may be expected even within the constraints of the QSHOD models, a point that has apparently escaped previous notice.

While the adequacy of the QSHOD models will be questioned later (see also Ref. 11, 38, 46 and 47), it is appropriate to consider first the completeness and validity of past applications using those models. Much of the earlier work on BMI relates to the effect of combustor pressure. Recalling that the constants A and B in the models are relatively pressure independent (Ref. 39), the effect of pressure enters in only through the mean burning rate, \bar{v} , in the variables A , L^* and Ω (i.e., the solutions in Fig. 4.2 are each valid for all pressures with the different curves presumably representing different propellants). The detailed behavior as a function of pressure can then be examined in any desired context by use of the appropriate curve in Fig. 4.2 and the relevant steady-state burning rate-pressure dependence of the propellant wherever burning rate appears in A , L^* and Ω . As an example, the

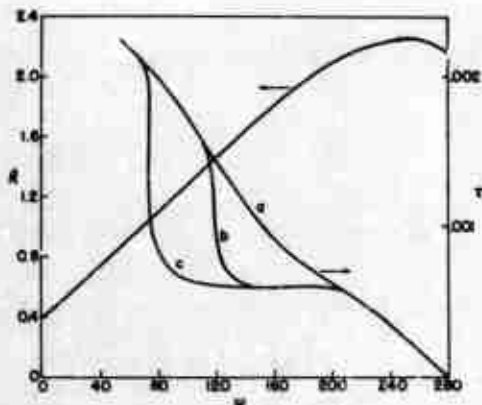


FIG. 4.1a. R and τ Functions for Pressure Response to Combustion Perturbations. Curves b and c show deviations from the usually accepted trend, suggested by test results shown in Fig. 4.3 and 4.4.

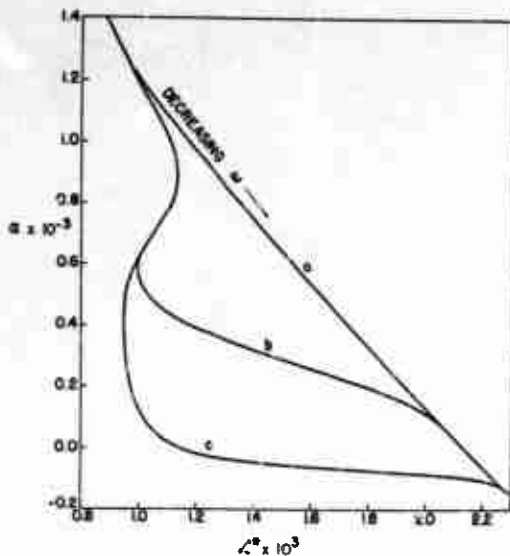


FIG. 4.1b. Solutions to Eq. 4.1 and 4.2 Corresponding to the R and τ Functions in Fig. 4.1a.

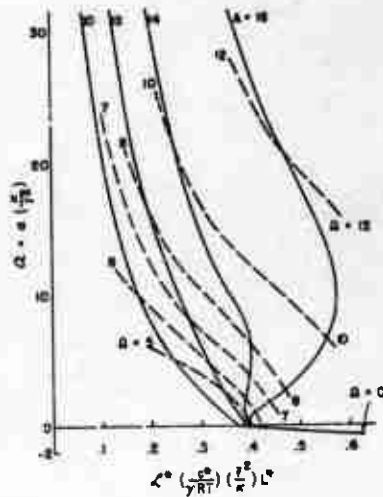


FIG. 4.2. Solutions to Eq. 4.1 and 4.2 for Response Functions From QSHOD Combustion Model With Various Values of the Parameter A (Which is Related to the Kinetics of the Surface Decomposition Reactions). The value of the parameter B in Eq. 5.1 used here was 0.8.

stability limit $\alpha = 0$ corresponds to specific values of $\Omega = \kappa \omega / \bar{r}^2$ and $L^* = \kappa \phi L^* / \bar{r}^2 c^*$ for any particular curve in Fig. 4.2, i.e.,

$$\omega_{\alpha=0} = (\Omega_{\alpha=0} / \kappa) \bar{r}_{\alpha=0}^2 = (C^2 \Omega_{\alpha=0} / \kappa) \bar{p}_{\alpha=0}^{-2n} \quad (4.3)$$

$$L^*_{\alpha=0} = (c^* L^*_{\alpha=0} / \kappa \phi) \bar{r}_{\alpha=0}^2 = (C^2 c^* L^*_{\alpha=0} / \kappa \phi) \bar{p}_{\alpha=0}^{-2n} \quad (4.4)$$

where \bar{r}^2 was replaced on the right-hand side by a frequently used pressure dependence $\bar{r} = C p^n$ (see comment, Section 3.2). It is these two relations that have been used to correlate experimentally determined trends of BMI. Thus in Ref. 40, Eq. 4.4 was used to correlate stability limit data in terms of \bar{p} and L^* , while data relating ω to \bar{r} and \bar{p} were correlated with the stability limit defined by Eq. 4.3 in Ref. 36, 38 and 42. This is a rather superficial treatment of both theory and experiment, which contain much more of value than the functional form of the $\alpha = 0$ stability limit.

4.2. TROUBLES WITH PRESENT STATUS OF KNOWLEDGE

There are several aspects of the present situation that seem to be blocking further progress. One is the preoccupation with stability limits. Most experiments yield measurements of α , ω , L^* , \bar{p} and \bar{r} , and these measurements can be correlated in a variety of ways that are more meaningful than mere verification of a stability limit. As an example, values of R and τ can be calculated, and in principle a portion of the response function curve can be determined. Only limited efforts along these lines have been reported (Ref. 36 and 39). Even in the discussions of stability limits, undue reliance is made on the results provided by the QSHOD models (Eq. 4.3 and 4.4). The resulting comparisons between experiment and analysis are sometimes quite unsatisfactory (Ref. 11, 38 and 46). A particularly good example is provided by BMI studies (Ref. 38) of two similar propellant formulations in which the principal difference was between the polyurethane and CTPB binders. The stability limit trends predicted by the QSHOD theory were in agreement with the results from the CTPB propellant, but in sharp disagreement with the results from the polyurethane propellant.

A second problem with recent literature concerns the use of the criterion $\alpha = 0$ to define the stability limit. This criterion defines a minimum frequency Ω below which $\alpha < 0$ so that oscillations do not grow. It can be seen from Fig. 4.1 and 4.2 that the maximum value of L^* for oscillatory behavior sometimes corresponds to $\partial\alpha/\partial L^* = \infty$ rather than $\alpha = 0$. This point apparently has not been noticed in previous discussions of stability limit, although the behavior when L^* is near this limit is qualitatively different from the $\alpha = 0$ case and may explain some of the disagreement between theory and experiment noted in earlier work (Ref. 11, 38, 46 and 47). Within the QSHOD "theory" the principal difference is the finite value of α at the stability limit (the pressure dependence remains as in Eq. 4.3 and 4.4). Outside the QSHOD theory, it may happen that a gradual transition from Type s to Type b to Type c behavior (Fig. 4.1b) occurs as a function of a test variable such as pressure, with a corresponding shift from an $\alpha = 0$ type of stability limit to a $\partial\alpha/\partial L^* = \infty$ type of stability limit. A review of certain data from Ref. 38 seems to support this interpretation (Fig. 4.3). In this work, tests at low pressures yielded values of α decreasing to zero as L^* increased, suggestive of curve s in Fig. 4.1b. As pressure was raised, it became increasingly difficult to obtain low values of α , suggestive of a trend towards a stability solution like curve c in Fig. 4.1b (under these conditions, when testing in the L^* range where $\alpha \rightarrow 0$ on the lower branch of curve c, oscillations would be expected to be observed instead at the higher frequency and α corresponding to the upper branch of the α - L^* curve). The behavior at higher pressure is thus suggestive of stability limit behavior corresponding to $\partial\alpha/\partial L^* = \infty$, not previously considered in the literature. The trend from an $\alpha = 0$ to a $\partial\alpha/\partial L^* = \infty$ type of stability limit as pressure increases cannot be encompassed within the QSHOD model-dependent analyses because the corresponding form of the A versus L^* curves (Fig. 4.2) are relatively insensitive to pressure in the QSHOD model.

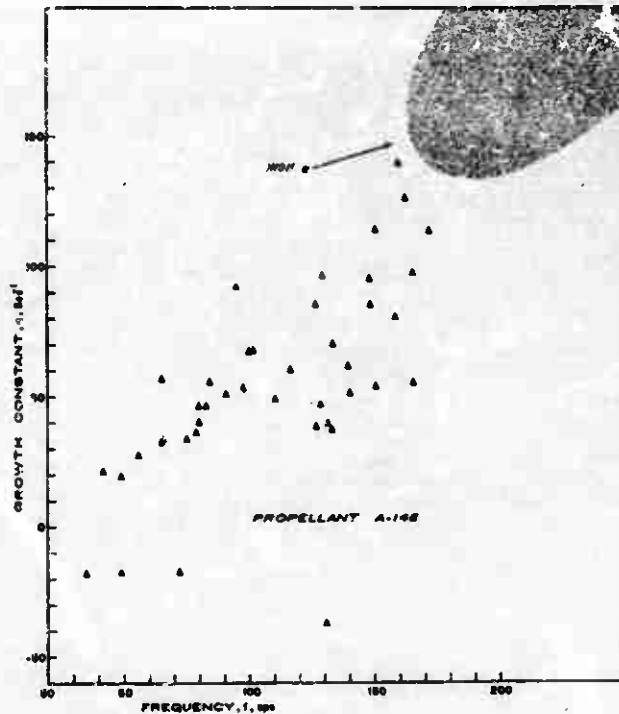


FIG. 4.3. Data from BMI Tests on A-146 Propellant (75% Bimodal AP, 25% Polyurethane Binder). Trend of data suggests a transition from $\alpha = 0$ type stability limit for low frequency (low pressure, curve A (Fig. 4.1b)) tests, to $\partial\alpha/\partial L^* = \infty$ type of stability limit in high frequency (high pressure, curve B (Fig. 4.1b)) tests. Low values of α could not be obtained at high frequency or pressure.

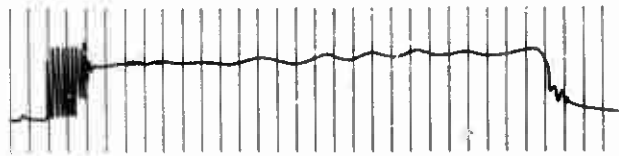


FIG. 4.4. Test Record With Transition in Oscillation Frequency Suggestive of L^* Increasing Through Cross-over Point in Stability Curve of Type C (Fig. 4.1b).

Figure 4.4 provides an interesting (and previously enigmatic) test of the perturbation equations (Eq. 4.1 and 4.2). In this test, as the L^* increased during burning, the system exhibited a spontaneous abrupt transition from high frequency to low frequency oscillations. This behavior is easily explained in terms of curve b of Fig. 4.1b, where severe high frequency oscillations are to be expected for low L^* . A $\partial\alpha/\partial L^* \rightarrow \infty$ type "stability" limit is reached, beyond which oscillations would be expected at some lower frequency corresponding to the lower, high L^* section of the solution curve. From an examination of Fig. 4.2, it appears that this behavior is not consistent with the QSHOD combustion perturbation models because for those models the lower branches of the solution curves are at negative α . It is the "anomaly" in the τ versus ω curve (in Fig. 4.1a) that causes the multiple valued functions in Fig. 4.1b. In view of the similar qualitative nature of the α - L^* curves in Fig. 4.2, and in view of test results such as illustrated by Fig. 4.4, it seems entirely plausible that solutions to Eq. 4.1 and 4.2 with real response functions may have the form of curve b in Fig. 4.1b.

From the foregoing it is evident that there is much to be learned by considering the entire solution to Eq. 4.1 and 4.2, instead of just the stability limits. Further, it seems clear that the QSHOD models for perturbation combustion are qualitatively incorrect. Because of the limitations of the QSHOD model, attention has been turned to a more detached study of the structure of the combustion zone. Motion pictures of burning samples, and SEM pictures of quenched samples have revealed in considerable detail the nature of the burning surface (see earlier section of this report). It consists (at low pressures typical for BMI) of an array of oxidizer particles protruding from the pyrolyzing binder. It must be presumed that under oscillatory conditions, these oxidizer particles will respond in a different way than will the binder, with resultant oscillation in mixture ratio of gases coming from the combustion zone. Such processes are not encompassed in the QSHOD perturbation models of combustion. Some success (Ref. 38) has been realized in an alternate scheme for correlating BMI stability limit data, a scheme in which the natural time constant for combustion oscillations is assumed to be the time to repopulate the burning surface with oxidizer particles once the population has been perturbed. This time constant is the time to burn the distance of an oxidizer particle diameter. For some propellants, the BMI data has been better correlated as a function of pressure and oxidizer particle size by this "layer" concept than by QSHOD models.

The view that the QSHOD models are sometimes even qualitatively inaccurate is supported not only by the foregoing examples, but also by substantial additional experimental evidence (Ref. 11, 38, 46 and 47). Continued reliance upon them appears to be blocking full and correct interpretations of BMI experiments. The analytical convenience of the QSHOD model is unfortunately also an intellectual straitjacket. It may be that reproducibility of BMI tests is too poor to make full interpretation satisfying, or the applicability of Eq. 4.1 and 4.2 may merit some scrutiny, but the most promising line of inquiry seems to be an escape from QSHOD model-dependent stability limit correlations to a more complete and less inhibited interpretation of results.

5. ACOUSTIC INSTABILITY

Studies of wave mode instability have continued along three lines. The dynamic response of the combustion zone to perpendicularly incident pressure waves has been studied by both analytical modeling and measurements of detailed combustion zone behavior. The net effect of this pressure-coupled combustion response in amplifying pressure waves was studied experimentally using the T-burner, with several propellant formulations. Finally, a continuing effort was devoted to testing the pressure-coupled response of propellants used in development programs, with the purposes of providing advance warning of risk, and evaluation of relevance of the laboratory tests to observed motor behavior.

5.1. ANALYTICAL MODELING OF PRESSURE COUPLING

A survey of one-dimensional models of pressure-coupling was presented in an earlier report. This work was rewritten, updated,¹ and to some extent simplified during the present reporting period, and was published as a survey paper in a technical journal (Ref. 39). This work was more successful than originally anticipated, in that it provided the principal results of all previous models in terms of a single functional form for the burning rate response function,

$$\frac{m'/m}{p'/p} = \frac{n_{AB} + n_s (\lambda - 1)}{\lambda + (A/\lambda) - (1 + A) + AB} \quad (5.1)$$

In this expression the left-hand side is essentially the amplification factor for incident pressure waves. The values of the quantities A, B and n_s depend upon fundamental aspects of the combustion such as activation energies, and λ is a function of the normalized frequency of oscillation. From this relation it is easy to determine the relative contribution of the various reaction steps to instability in terms of the parameters A, B, and n_s , assuming those parameters are known. More recent work, described in this report, has been focused on elucidation of the processes determining the parameters A, B, and n_s and on development of more rigorous modeling of the combustion response.

¹ Work funded partly from Naval Ordnance Systems Command Task No. UF 19.332.330.

One of the more conspicuous aspects of the models represented by Eq. 5.1 is a "persistent" prediction that the maximum value of the response function $(m'/m)/(p'/p)$ is relatively insensitive to pressure, and that the maximum occurs at a frequency of pressure oscillation that is a function of burning rate,

$$\omega_{\max} = r^2 \quad (5.2)$$

This point is mentioned here because the experimental results reported below are in sharp contrast to this prediction.

While it will no doubt be necessary to go to more complicated modeling of the combustion zone if accurate predictive capability is to be achieved, there are some rather elementary extensions of the present models that would enhance their relevance. One of the principal weaknesses of previous models has been in representation of the heat transfer to the burning surface from the gas phase. This has in most cases been contained in the undetermined parameter "B" in Eq. 5.1, and in all cases has been based on the assumption that the response of the gas phase during oscillations was quasi-static. In one case where B was not treated in a completely parametric way, it was assumed (Ref. 11) that the gas phase reaction started at the surface, and remained at constant rate until the reactants were consumed. The analytical model was extended during this reporting period to encompass a more realistic representation of the distribution of the gas phase reactions, and a calculation was also made of the limitations of the quasi-static approximation for the gas phase combustion. These developments are reported fully in Ref. 18. The results indicate that the surface-attached gas phase reaction zone model used by Krier, et al, (Ref. 52) gives significantly different results than a model in which some stand-off of the flame is allowed. Examination of the effect of the quasi-static assumption shows that it does not materially affect the prediction of the in-phase component of combustion response to pressure in the frequency range up to 10,000 cps, but does cause error in calculation of the magnitude and phase of the overall combustion response at high frequency. These results presumably improve the prospects of correlation of experiments with theory, but the experimental work on combustion zone structure indicates that still more complicated models will be required before fully satisfactory agreement will be obtained between experiment and theory. Existing models may have some predictive capability for trends. One remaining extension of the one-dimensional theory is the nonlinear analysis, which is currently in progress.

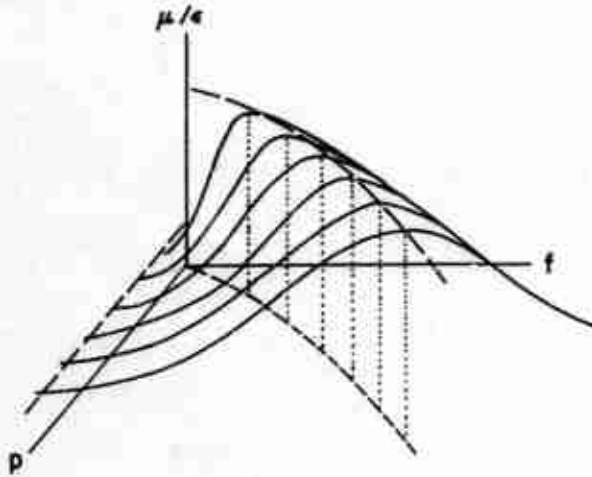
5.2. MAPPING RESPONSE FUNCTION OF PROPELLANTS

One of the long-time goals of experimental research on combustion instability has been to characterize the perturbation behavior of propellants over the entire domain of pressure and frequency for which

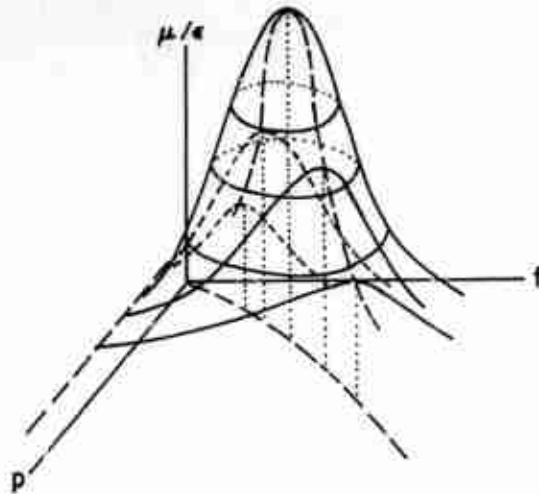
instability is possible. In the present program, extensive effort has been devoted to development of experimental techniques for this purpose, but each technique has been amenable to only a restricted range of conditions of interest. During the past year, tests have been completed on certain propellants over the range of conditions accessible to three experimental systems. The response function was measured in the high-frequency domain using the 1.5-inch diameter T-burner (Ref. 47 and 49), and in the low frequency domain using the 5.5-inch diameter T-burner (Ref. 1, 2, 4, 5, 50 and 51), and the 1.5-inch diameter L* burner (Ref. 1-5, 27, 38 and 50). The results of these studies were reported at the Twelfth Combustion Symposium (Ref. 46), and will appear in the published volume of the meeting. The results are summarized briefly here.

Studies were made of four propellants, designated A-13, A-35, A-91 and A-148. A-13 consists of a 76-24% mixture of 80 μ AP and PBAN binder, A-35 consists of a 75-25% mixture of 80 μ AP and polyurethane binder, and A-91 consists of a 67-25-8% mixture of 80 μ AP, polyurethane binder and 80 μ aluminum. A-148 is a 75-25% mixture of bimodal AP (50/50 mixture of 15 μ and 200 μ particle sizes) and polyurethane binder. The test results were summarized in the form of contour maps of the in-phase component of the response function (μ/ϵ), plotted in the pressure-frequency plane.

Recalling the discussion in the last section, the one-dimensional perturbation theories predict that the response function "surface" above the p-f plane should be a ridge of roughly constant height (Fig. 5.1a), with the corresponding constant- μ/ϵ lines in the p-f plane being open curves following the trend of the ridge of the response function surface. The experimental results did not conform to this trend (Fig. 5.2), indicating the need for more realistic modeling of the combustion process. All four propellants showed behavior suggestive of a "peaked" response function surface (Fig. 5.1b) instead of a ridge, with the location and height of the peak depending on the propellant composition. A-13 propellant (PBAN binder) showed a broad peak centered around 300 psia and 300 cps (Fig. 5.2a). A-35 propellant (polyurethane binder) showed a peak centered around 70 psia and 60 cps (only roughly determined), with magnitude comparable to that of Fig. 5.2b. The "bimodal" formulation A-148 gave similar trends (Fig. 5.2c) with no singular behavior currently attributable to the bimodal oxidizer particle size distribution. The response function contours are open in Fig. 5.2c because the unstable region extended into the region of atmospheric pressure where testing was not feasible. The polyurethane formulation with 8% aluminum (A-91) showed a very high, localized peak in the region of 30 psia and 15 cps (Fig. 5.2d), a result that confirmed previous qualitative interpretations to the effect that the metal combustion can produce a "preferred frequency" type of instability (Ref. 1-4 and 51) that can be quite severe under rather specialized conditions. The results also indicate that instability problems tend to be more serious at low frequencies and low pressures, although results with other propellants indicate that the examples shown here "peak out" at lower pressure and frequency than the average.

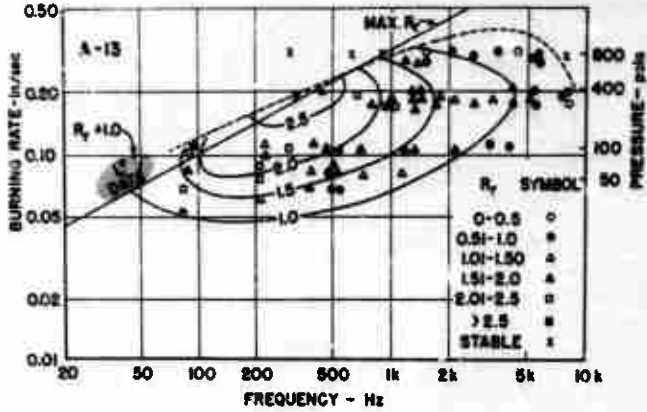


(a)

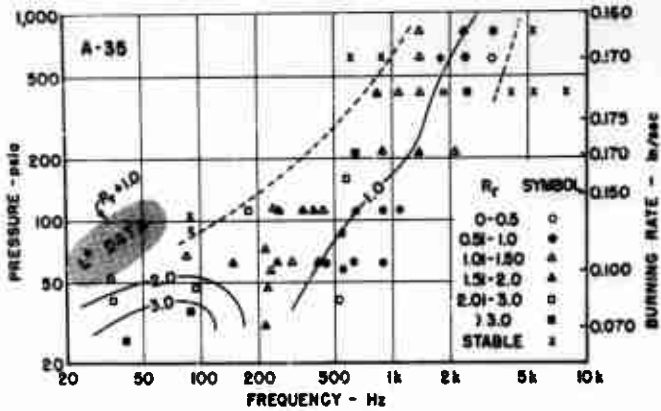


(b)

FIG. 5.1. (a) Response Function Surface Above the Pressure-Frequency Plane as Predicted by One-dimensional Perturbation Theories. (b) Idealized Representation of the Response Function Surface Above the Pressure-Frequency Plane as Determined by Experimental Measurement.

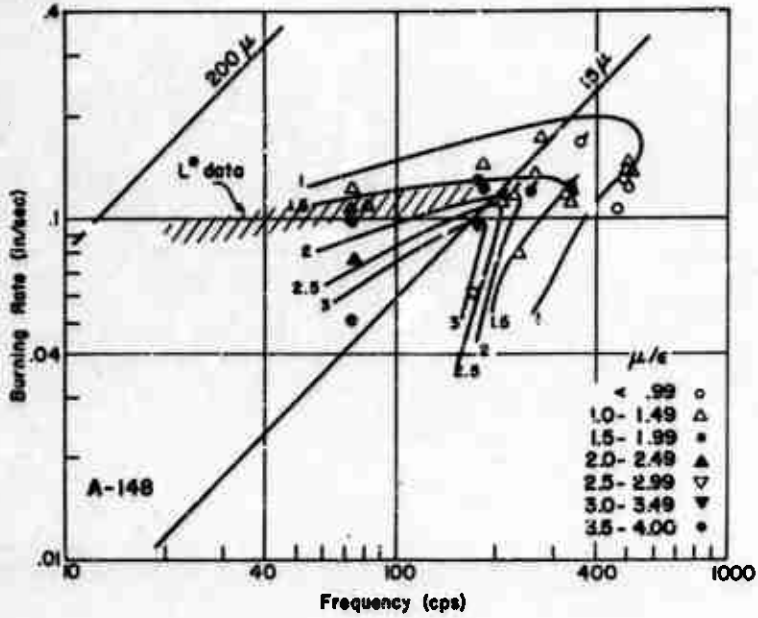


(a) A-13 Propellant

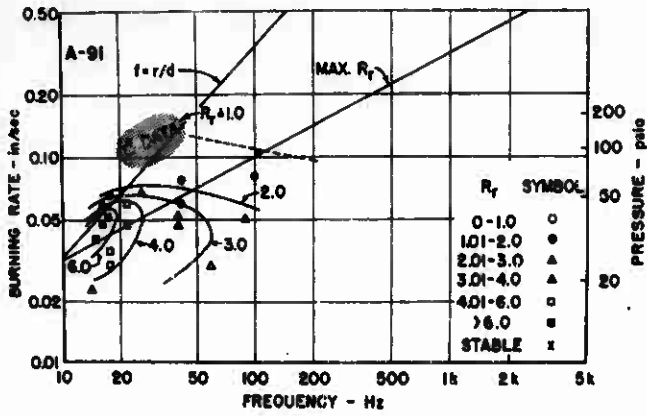


(b) A-35 Propellant

FIG. 5.2. Contour maps of the In-Phase Component (Real Part) of the Response Function of Four Propellant Compositions.



(c) A-148 Propellant



(d) A-91 Propellant

FIG. 5.2 (Cont'd.).

5.3. OBSERVATIONS OF COMBUSTION ZONE DYNAMICS

Direct observation of combustion zone dynamics is seldom possible, yet knowledge of combustion zone dynamics is vital to an understanding of phenomena involved in acoustic instability and to the construction of correct mathematical models. Most of our knowledge of combustion zone dynamics is obtained through indirect evidence. The NVC 5.5-inch diameter DECEV (T-burner) is being used as a tool to delve into certain aspects of combustion zone dynamics. Although events occurring in the combustion zone are inferred from observations of the combustion products as they flow away from the propellant surface, several advances have been made in understanding these complicated phenomena. The 5.5-inch DECEV has been instrumented with a variety of devices in addition to the usual pressure transducers, which include multiple radiation transducers to detect metal combustion clouds (Ref. 4), a slit window and camera for space-time recording of gas motion (Ref. 5), and high speed gas temperature measurements (Ref. 5).

Earlier difficulties were encountered in interpreting streak photographs of the gas motion in the burner (Ref. 5). These were largely surmounted during the present reporting period by moving the propellant to a position initially at one end of the slit window, by correcting the image exposure on the film, and by completing the development of a mathematical model which describes gas flow in the burner (Ref. 6). The mathematical model was programmed for digital computer and solutions compared with streak photographs of gas motion in the burner. The comparison shows that the model provides a reasonably accurate description (see Fig. 4.1 in Ref. 6).

Early streak data indicated that temperature variations in the flow arose from an apparent flame temperature variation as well as the predicted entropy variations (Ref. 5). Measurements of temperature oscillations near the propellant surface gave results that in some cases were much larger than could be accounted for by isentropic compression of the gas. Although the greater values might be explained by a dependence of the flame temperature on pressure, measurements of the temperature under nonoscillating conditions and calculation of the dependence of temperature from equilibrium data tend to discount this explanation. Another explanation was sought along the line of changing gas stoichiometry caused by differential changes in burning rate of the propellant constituents with pressure. A series of calculations was made on a digital computer for a hypothetical propellant with several fuel to oxidizer ratios and chamber pressures. The calculated flame temperatures are plotted in Fig. 5.3. Several significant conclusions can be drawn from the data: (1) The temperature is most sensitive to the fuel-oxidizer ratio in the region representing propellants being investigated (75% oxidizer), (2) the temperature is least sensitive to changes in mean pressure in this same region, (3) the sensitivity of temperature to changes in fuel-to-oxidizer ratio in the 70% to 80% oxidizer region is sufficient (over 100°K for a one percent oxidizer change) to explain the excessive temperature excursions noted earlier.

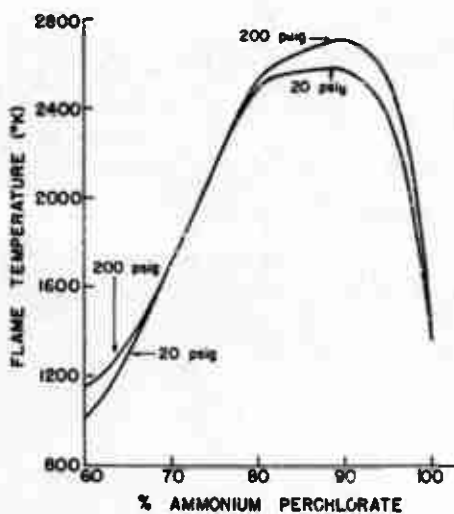


FIG. 5.3. Dependence of Flame Temperature on Percent Oxidizer and on Pressure for NH_4ClO_4 -Estane Propellants.

Numerous problems remain unsolved in this subject area. Some of the points mentioned below are interrelated but a partial list includes:

1. Attempt characterization of the combustion zone, particularly its extent into the flow field, which may be considerable when dealing with metallized propellants.
2. Measure temperatures at known distances from the propellant surface to: (a) verify that the theoretical model of gas flow in the burner provides an adequate description of events; (b) use data, when point (a) is confirmed, to extrapolate back to the combustion zone to calculate flame behavior.
3. Gather evidence to support or deny "mixture ratio" hypothesis.
4. Apply standard and time-resolved spectroscopy to study optical emissions from combustion gases to: (a) identify general nature of emission, (b) study the nature of reactions in the combustion zone, (c) determine the spatial extent of combustion zone, (d) map distribution of chemical species in space and time and attempt to infer combustion zone dynamic behavior.

5. Extend studies to higher pressures and frequencies.
6. Develop more adequate means for study of metal combustion and the role of metal in combustion oscillations.

5.4. TESTING OF PROPELLANTS FROM DEVELOPMENT PROGRAMS

Four propellants from the Jet Propulsion Laboratory were evaluated for combustion characteristics. These propellants contained a "saturethane" binder and were designed to withstand the high temperature conditions necessary to biologically sterilize the apparatus containing the propellant. They were evaluated in the photographic strand bomb and in the NWC 1.5-inch diameter T-burner. Two of the compositions were non-metallized, one contained 1/2% powdered aluminum, and the fourth had 2% aluminum.

Color photography of the combustion zone showed somewhat more molten binder than with NWC polyurethane compositions. T-burner testing on the propellants showed moderate instability for the two unmetallized compositions in the mid-range of pressure and frequency (see Fig. 5.4). Acoustic response function values were moderately low in the range tested and acoustic instability appears unlikely in the motor design currently being considered by this propellant.

A few preliminary tests in the L*-burner resulted in oscillatory behavior at extremely low L* and pressure. Nonacoustic instability would seem unlikely in the L*-pressure range of the current motor design.

Two compositions were received from Thiokol Chemical Co. and were tested in the NWC 1.5-inch T-burner. Both showed moderate instability. One of these was a heavily metallized composition with a high-energy oxidizer. In the four cases where this propellant was unstable, the response function was of the order of unity or less in three tests and was less than two on the other test. These are only moderate values of the response function, in spite of the fact that the growth and decay rates of the oscillations were of somewhat greater magnitude than usually encountered. A relatively high flame temperature and burning rate appear to be the principal factors causing the instability of this propellant, which is capable of producing high growth α 's even in the presence of the high attenuation (high decay α) resulting from the aluminum oxide smoke. The likelihood of acoustic instability with this propellant in the proposed application was judged to be moderately low for axial modes and somewhat higher for transverse modes. As in all cases, precise prediction of motor stability from T-burner results is not possible because the gain-loss characteristics of the motor are extremely difficult to determine and the influence of gas perturbations parallel to the burning surface is not tested in the T-burner.

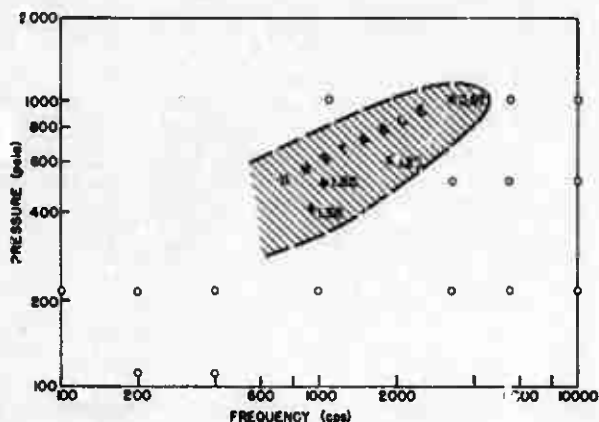


FIG. 5.4. Acoustic Instability Behavior of a JPL "Saturrethane" Propellant. Open symbols represent stable tests, solid symbols denote unstable behavior. Numbers indicate values of the in-phase component of the response function. The approximate region of T-burner instability with this propellant is indicated by the shaded area.

As a result of instability troubles in a motor under development, six candidate propellant compositions were sent by Aerojet-General Corp., which were tested in the 5.5-inch diameter T-burner at a nominal frequency of 380 cps. Only three tests of each propellant were made due to shortage of material. Two tests series were at ambient temperature and the final one was with propellant at approximately 150°F. No instability was noted for any of the compositions at any condition. Photographic strand bomb results, however, showed a wide variety of aluminum behavior. It seems likely that the instability encountered in the motor was due primarily to velocity-coupled mechanisms rather than to pressure-coupled phenomena.

6. ACOUSTIC ATTENUATION

Stability of solid propellant combustors is primarily a consequence of attenuation of flow disturbances by viscous processes and by convection through the nozzle. Because of the difficulty of calculating these processes in combustors of complicated geometry, a cold-flow experimental technique was developed which would permit determination of the effect of geometrical variables on losses in axial modes of combustor models. This work was reported previously (Ref. 8, 9, and 53). Experimental work during the present reporting period has been limited to attenuation measurements incidental to T-burner testing, the cold-flow work having been discontinued due to reduced funding.

An analytical study was completed concerning the interpretation of cold-flow experiments. This study, entitled "An Analysis of Axial Acoustic Waves in a Cold-Flow Rocket", has been reported fully in Ref. 10 and will be discussed only briefly here. In the study, equations were derived for steady state or driven oscillations and for freely decaying waves. The analysis was motivated by an uncertainty regarding the quantitative validity of the "half power bandwidth" method used in determining the attenuation alphas from resonance curves obtained from the cold-flow tests. The analysis showed that the method was applicable to cases where the effective admittance of the nozzle end of the motor was small and the motor geometry relatively simple. For more "lossy" motors an alternative method was provided in which the acoustic attenuation may be obtained graphically from plots of the effective nozzle admittance dependence on resonant frequency and half power bandwidth.

7. CONSULTING AND REPORTING

An appreciable amount of time was spent during this reporting period on various consulting and reporting activities that would be regarded as "bridging the gap" between research and application. These activities are summarized briefly below:

7.1. CONSULTING ON DEVELOPMENT PROGRAMS

A review of development and proposed application of saturethane propellants was made for the Jet Propulsion Laboratory/California Institute of Technology (JPL/CIT), relative to the likelihood of problems with combustion instability. Tests were made of samples of propellant supplied by JPL/CIT, tests including window bomb photography, T-burner firings and nonacoustic burner tests. From the results of these studies it was concluded that the susceptibility of the saturethane propellants tested to combustion is relatively low; nonacoustic instability is a possibility, but only at lower pressure and L^* than called for in present designs.

Oscillatory behavior (axial mode) in development-1 static firings of the motor for the Navy Standard Missile was reviewed and recommendations made for modification of oxidizer and aluminum particle size in the propellant and a minor change in charge design. The changes led to stable behavior.

Axial mode oscillatory behavior in a Rocketdyne advanced motor for Redeye was studied and burner tests were conducted on a family of propellants with variations in oxidizer and aluminum particle size distribution. The objective of these studies (insofar as the NASA program is concerned) was to determine the relevance of laboratory tests to actual motor behavior. This particular motor represents a motor test situation (aluminized propellant, axial mode oscillation, frequency 600 cps) in which only limited success has been achieved in laboratory testing methods. In this case, the window bomb photography showed considerable difference in steady-state combustion behavior among the propellants tested, but motor testing was confined (for separate reasons) to a subset of propellant formulations whose combustion in the window bomb appeared similar. All were unstable in rocket motor firings. Extensive testing is being done in a 5.5-inch diameter T-burner. Oscillations do not occur spontaneously, presumably because of high attenuation by Al_2O_3 smoke. A pulse-decay technique used previously for low frequency instability testing is being adapted to this 600 cps range.

In cooperation with Thiokol Chemical Corporation and the Air Force Rocket Propulsion Laboratory, tests (T-burner) were run on several propellant formulations using hydrazine dimerchlorate as the oxidizer. The testing work was done on a Navy program, but is mentioned here because of its fundamental importance. These propellants are unusually unstable at the high frequencies tested, and formulations with up to 4% aluminum were still very unstable. Although this and other test work has shown a serious problem with instability, it should be noted that no information has yet been obtained at the frequencies characteristic of motors of operational size. Thus the unfavorable results may lead to unjustified concern with this problem. In another respect the combustion instability problem with HP_2 is of continuing interest: why are HP_2 propellants so unstable? The answer to that question may reveal much about the detailed mechanisms of instability.

Another development program that has encountered a significant degree of oscillatory combustion is the Minuteman 3rd Stage Wing II. This experience was reviewed with personnel of Hercules Powder Company, and discussions are continuing. The behavior involves axial mode oscillations at about 500 cps. The principal interest to NASA is the fact that this motor is similar to high performance "space" motors NASA might use, with a heavily aluminized propellant, low operating pressure, and high volumetric loading.

Axial mode oscillatory behavior was encountered in static development tests on an advanced motor for Sparrow, at frequencies in the 400-1200 cps range. In consultations on this program it was recommended that a Helmholtz resonator attenuator be used in the motor. Tests to date have shown the attenuator to be effective.

A general comment on the above and other recent experience with combustion instability is needed. Most recent problems have been in the 100-1200 cps range, in axial modes, with heavily aluminized propellants. There is a wide-prevailing misconception that large motors and motors with heavily aluminized propellants are inherently stable. While most information supports these views relative to the big booster motors, it is absolutely clear that it is not true for intermediate size boosters and upper stages. There are two programs in which oscillatory behavior at 80 cps has occurred. In other development programs it has been repeatedly observed that this axial mode instability can occur consistently in rather innocuous form and then undergo transition to violently unstable behavior because of small propellant or design changes, or flow disturbances due to discharge of debris through the nozzle. Thus increasing attention to this class of behavior is needed.

7.2. SURVEY AND EDUCATIONAL ACTIVITIES

Efforts have continued to organize knowledge in the field of combustion instability and present it in a form conducive to more widespread application. A survey paper was prepared and presented at the Twelfth Combustion Symposium (Ref. 54), summarizing recent developments in

research. A tutorial paper was presented at the Third ICRPG/AIAA Solid Propulsion Meeting, summarizing the nature, prevalence and scientific basis of combustion instability, and this paper is being expanded for publication through CPIA. A two-day seminar was presented on the topic of solid propellant combustion, under the auspices of the American Institute of Aeronautics and Astronautics. This course drew heavily on results from the present program, including a tutorial presentation of ingredient decomposition, steady state combustion, instability and ignition. Copies of the course notes are available from AIAA Headquarters (Ref. 28). The material is currently being rewritten and expanded into a book.

7.3. SUPPORT OF THE INTERAGENCY CHEMICAL ROCKET PROPULSION GROUP

Activities in this area have included chairmanship of the Solid Propellant Combustion Working Group, organization of a tutorial session at the Third ICRPG/AIAA Solid Propulsion Meeting, membership in and support of the "T-Burner Standardization" Committee and the "Arc-Image Ignition Standardization" Committee, and initial planning of a working meeting on ammonium perchlorate decomposition (for April 30, 1969).

7.4. SUMMARY OF REPORTS

A list of publications pertaining to work on this program is enclosed as Appendix A.

Appendix A

LIST OF PUBLISHED REPORTS DURING
THIS REPORTING PERIOD

1. Beckstead, M. W., and E. W. Price. Nonscoustic Combustor Instability, AMER INST AERONAUT ASTRONAUT J, Vol. 5, No. 11 (November 1967), pp. 1969-96.
2. Beckstead, M. W., and T. L. Boggs. The Effect of Oxidizer Particle Size on Nonacoustic Instability, in 4th Combustion Conference, Interagency Chemical Rocket Propulsion Group, comp. and ed. by Chemical Propulsion Information Agency. Silver Spring, Md., CPIA, December 1967. CPIA Publ. No. 162, Vol. 1, pp. 337-46.
3. Beckstead, M. W., and P. E. C. Culick. A Comparison of Analysis and Experiment for the Response Function of a Burning Surface, in 4th Combustion Conference, Interagency Chemical Rocket Propulsion Group, comp. and ed. by Chemical Propulsion Information Agency. Silver Spring, Md., CPIA, December 1967. CPIA Publ. No. 162, Vol. 1, pp. 331-36.
4. Hightower, J. D., E. J. Price, and D. E. Zuru. Continuing Studies of the Combustion of Ammonium Perchlorate, in 4th Combustion Conference, Interagency Chemical Rocket Propulsion Group, comp. and ed. by Chemical Propulsion Information Agency. Silver Spring, Md., CPIA, December 1967. CPIA Publ. No. 162, Vol. 1, pp. 527-34.
5. Kraeutle, K. J. The Decomposition of Crystalline and Granular Ammonium Perchlorate, in 4th Combustion Conference, Interagency Chemical Rocket Propulsion Group, comp. and ed. by Chemical Propulsion Information Agency. Silver Spring, Md., CPIA, December 1967. CPIA Publ. No. 162, Vol. 1, pp. 535-43.
6. Price, E. W. Solid Propellant Combustion: State of Knowledge 1967. China Lake, Calif., NWC, April 1968. (NWC TP 4520).
7. Aerothermochemistry Division. Combustion of Solid Propellant and Low Frequency Combustion Instability, Progress Report, 1 April-30 September 1967. China Lake, Calif., NWC, April 1968. (NWC TP 4478).
8. Culick, P. E. C., and G. L. Dehority. An Analysis of Axial Acoustic Waves in a Cold-Plow Rocket. China Lake, Calif., NWC, May 1968. (NWC TP 4544).

9. Beckstead, M. W., and F. E. C. Culick. A Comparison of Analysis and Experiment for Solid Propellant Combustion Instability. China Lake, Calif., NWC, May 1968. (NWC TP 4531).
10. Culick, P. E. C. Some Nonacoustic Instabilities in Rocket Chambers Are Acoustic, AMER INST AERONAUT ASTRONAUT J, Vol. 6, No. 7 (July 1968), pp. 1421-23.
11. Price, E. W. Review of the Combustion Instability Characteristics of Solid Propellants, in "Advances in Tactical Rocket Propulsion, ACARD Conference Proceedings No. 1, April 1965." ed. by S. S. Penner. Maidenhead, England, Technivision Services, August 1968. Pp. 141-94.
12. Beckstead, M. W. Low Frequency Instability: A Comparison of Theory and Experiment, COMBUST AND FLAME, Vol. 12, No. 1 (October 1968), pp. 417-26.
13. Hightower, J. D., and E. W. Price. Experimental Studies Relating to the Combustion Mechanism of Composite Propellants, ASTRONAUTICA ACTA, Vol. 14, No. 1 (November 1968), pp. 11-21.

PUBLISHED SINCE REPORTING PERIOD
COVERED BY THIS REPORT

1. Culick, F. E. C. A Review of Calculations for Unsteady Burning of a Solid Propellant, AMER INST AFRONAUT ASTRONAUT J, Vol. 6, No. 12 (December 1968), pp. 2241-55.
2. Mathes, H. B., T. L. Boggs, C. L. Dehority, and J. E. Crump. Low-Frequency Combustion Instability Progress Report, 1 October 1967-31 March 1968. China Lake, Calif., NWC, December 1968. 44 pp. (NWC TP 4565).
3. Culick, F. E. C. Some Problems in the Unsteady Burning of Solid Propellants. China Lake, Calif., NWC, February 1969. 68 pp. (NWC TP 4668).
4. Boggs, T. L. The Deflagration of Pure Single Crystals of Ammonium Perchlorate, New York, N. Y., American Institute of Aeronautics and Astronautics, 1969. AIAA Paper No. 69-142. 9 pp.
5. Boggs, T. L., J. L. Prentice, K. J. Kraeutle, and J. E. Crump. The Role of the Scanning Electron Microscope in the Study of Solid Propellant Combustion, in Proceedings of the 2nd Annual Scanning Electron Microscope Symposium, sponsored by IIT Research Institute, Chicago, Ill. (April 29-May 1, 1969), pp. 349-64.

6. Boggs, T. L., M. W. Beckstead, and O. H. Madden. The Effect of Oxidizer Particle Size and Binder Type on Nonacoustic Instability, New York, N. Y., American Institute of Aeronautics and Astronautics, 1969. AIAA Paper No. 69-175. 7 pp.
7. Price, E. W. Recent Advances in Solid Propellant Combustion Instability, Twelfth Symposium (International) on Combustion. Pittsburgh, Pa., Combustion Institute, 1968.
8. Beckstead, M. W., H. B. Mathis, E. W. Price, and F. E. C. Culick. Combustion Instability of Solid Propellants, Twelfth Symposium (International) on Combustion. Pittsburgh, Pa., Combustion Institute, 1968.
9. Price, E. W. Combustion Instability. Presented at the Third ICRPG/AIAA Solid Propulsion Conference in June 1968. To be published by CPIA.

REFERENCES

1. U. S. Naval Ordnance Test Station. Low Frequency Combustion Instability of Solid Rocket Propellants, 1 July - 1 September 1962, by E. W. Price. China Lake, Calif., NOTS, December 1962. (TPR 301, NOTS TP 3107), UNCLASSIFIED.
2. -----. Low-Frequency Combustion Instability of Solid Rocket Propellants, 1 September 1962 - 1 May 1963, by M. D. Horton, J. L. Eisel, and E. W. Price. China Lake, Calif., NOTS, May 1963. (TPR 318, NOTS TP 3248), UNCLASSIFIED.
3. -----. Low-Frequency Combustion Instability of Solid Rocket Propellants, by E. W. Price, D. W. Rice and J. E. Crump. China Lake, Calif., NOTS, July 1964. (TPR 360, NOTS TP 3524), UNCLASSIFIED.
4. -----. Combustion of Solid Propellants and Low Frequency Combustion Instability, by Aerothermochemistry Division. China Lake, Calif., NOTS, June 1967. 244 pp. (NOTS TP 4244), UNCLASSIFIED.
5. Naval Weapons Center. Combustion of Solid Propellants and Low Frequency Combustion Instability Progress Report 1 April-30 September 1967, by Aerothermochemistry Division. China Lake, Calif., NWC, April 1968. 108 pp. (NWC TF 4478), UNCLASSIFIED.
6. -----. Low-Frequency Combustion Instability Progress Report, 1 October 1967-31 March 1968, by H. B. Mathes, T. L. Boggs, G. L. Dehority, and J. E. Crump. China Lake, Calif., NWC, December 1968. 44 pp. (NWC TP 4565), UNCLASSIFIED.
7. -----. Decomposition and Deflagration of Ammonium Perchlorate, by T. L. Boggs and K. J. Kreeutle. China Lake, Calif., NWC, October 1968. 54 pp. (NWC TF 4630), UNCLASSIFIED.
8. U. S. Naval Ordnance Test Station. Acoustic Losses of a Subscale, Cold-Flow Rocket Motor for Various "J" Values, by F. G. Buffum, G. L. Dehority, R. O. Sistes, and E. W. Price. China Lake, Calif., NOTS, February 1965. 70 pp. (NAVWEPS Report 8971, NOTS TF 3932), UNCLASSIFIED.
9. -----. Operation Manual for the NOTS-NASA Rocket-Motor Acoustic Test Facility. Steady-State Resonance Tests With Flow, by F. G. Buffum, F. E. Werback, and D. R. Skar. China Lake, Calif., NOTS, June 1967. 36 pp. (NOTS TF 4304).

10. Naval Weapons Center. An Analysis of Axial Acoustic Waves in a Cold-Flow Rocket, by P. E. C. Culick and G. L. Dehority. China Lake, Calif., NWC, May 1968. 32 pp. (NWC TP 4544), UNCLASSIFIED.
11. -----, A Comparison of Analysis and Experiment for Solid Propellant Combustion Instability, by Merrill W. Beckstead and P. E. C. Culick. China Lake, Calif., NWC, May 1968. 30 pp. (NWC TP 4531), UNCLASSIFIED.
12. Hightower, J. D., and E. W. Price. Combustion of Ammonium Perchlorate, in "Eleventh Symposium (International) on Combustion." Pittsburgh, Pa., Combustion Institute, 1967. Pp. 463-72.
13. -----, Experimental Studies Relating to the Combustion Mechanism of Composite Propellants, ASTRONAUTICA ACTA, Vol. 14, No. 1 (November 1968), pp. 11-21.
14. Boggs, T. L. The Deflagration of Pure Single Crystals of Ammonium Perchlorate, New York, N. Y., American Institute of Aeronautics and Astronautics, 1969. AIAA Paper No. 69-142. 9 pp.
15. Beckstead, M. W., and J. D. Hightower. Surface Temperature of Deflagrating Ammonium Perchlorate Crystals, AMER INST AERONAUT ASTRONAUT J, Vol. 5, No. 10 (October 1967), pp. 1785-90.
16. Boggs, T. L., J. L. Prentice, K. J. Kraeutle, and J. E. Crump. The Role of the Scanning Electron Microscope in the Study of Solid Rocket Propellant Combustion. Proceedings of the Second Annual SEM Symposium, May 1-3 1969, Chicago, Ill., pp. 344-64.
17. Boggs, T. L., and K. J. Kraeutle. Role of the Scanning Electron Microscope in the Study of Solid Rocket Propellant Combustion, Part I, Ammonium Perchlorate Decomposition and Deflagration. To be published in the 2nd issue of COMBUSTION SCIENCE AND TECHNOLOGY.
18. Bobolev, V. K., A. P. Glaskova, A. A. Zenin, and O. I. Leypunsky. A Study of the Temperature Distribution in the Combustion of Ammonium Perchlorate, ZH PRIKL MEKHAN I TEKHNI PIZ, No. 3 (1964), pp. 153-58.
19. Friedman, R., R. G. Nugent, K. E. Rumbel, and A. C. Scurlock. Deflagration of Ammonium Perchlorate, in Sixth Symposium (International) on Combustion. New York, Reinhold, 1957. Pp. 612-18.
20. Levy, J. B., and R. Friedman. Further Studies of Pure Ammonium Perchlorate Deflagration, in Eighth Symposium (International) on Combustion. Baltimore, Williams and Wilkins, 1962. Pp. 663-72.

21. Glaskova, A. P. Effect of Pressure on the Combustion Rate of Ammonium Perchlorate, ZH PRIKL MEKHAN I TEKHN FIZ, No. 5 (1963), pp. 121-25.
22. Naval Weapons Center. Some Problems in the Unsteady Burning of Solid Propellants, by P. E. C. Culick. China Lake, Calif., NWC, February 1969. 68 pp. (NWC TP 4668), UNCLASSIFIED.
23. Culick, F. E. C., and G. L. Dehority. Elementary Calculations for Steady State Burning of Solid Propellants, Western States Combustion Institute Meeting, April 28-30 1969, China Lake, Calif. (Preprint WSS-69-7).
24. Baatres, E. K., K. P. Hall, and M. Summerfield. Modification of the Burning Rates of Solid Propellants by Oxidizer Particle Size Control. New York, American Rocket Society, 1961. (ARS Preprint).
25. Steinz, J. A., P. L. Stang, and M. Summerfield. The Burning Mechanism of Ammonium Perchlorate-Based Composite Solid Propellants, in ICRPG/AIAA 3rd Solid Propulsion Conference, Atlantic City, N. J., AIAA, June 1968. (Preprint 68-658)
26. Army Research and Development Group (Europe). The Prediction of the Burning Rate Exponent of Solid Propellants, by Robert J. Heaston. New York, N. Y. ARDG, December, 1966. (DDC Document AD 815882)
27. Summerfield, M., G. S. Sutherland, M. J. Webb, H. J. Taback, and K. P. Hall. Burning Mechanism of Ammonium Perchlorate Propellants, Solid Propellant Rocket Research, in PROG ASTRON ROCKETRY, Vol. 1 (1960), pp. 141-82.
28. Price, Edward W., and Fred E. C. Culick. Combustion of Solid Rocket Propellants, AIAA Professional Study Series (1968).
29. Lockheed Propulsion Company. Combustion Tailoring Criteria for Solid Propellants, by R. L. Derr and M. W. Beckstead, Redlands, Calif. Technical Report AFRPL-TR-68-191, Phase IV, October 1968. Technical Report AFRPL-TR-69-16, Phase V, January 1969.
30. Boggs, T. L., R. L. Derr, and M. W. Beckstead. Surface of Composite Ammonium Perchlorate Propellants. To be presented at the 4th ICRPG Solid Propulsion Conference 20 May 1969, Chicago, Ill.
31. Derr, R. L., and T. L. Boggs. The Surface Structure of Composite Propellants. To be presented at the AIAA 5th Propulsion Joint Specialists Conference 9-13 June 1968, Colorado Springs, Colorado.

32. Naval Weapons Center. Metal Particle Combustion Progress Report, 1 May 1967-30 September 1968, by J. L. Prentice and K. J. Kraeutle. China Lake, Calif., NWC, January 1969. 86 pp. (NWC TP 4658), UNCLASSIFIED.
33. Crump, J. E. Surface Characteristics of Quenched Samples of Composite-Aluminum Propellants, in 1st Combustion Instability Conference, Interagency Chemical Rocket Propulsion Group, comp. and ed. by Chemical Propulsion Information Agency. Silver Spring, Md., CPIA, January 1965. CPIA Publ. No. 68, Vol. 1, pp. 361-65.
34. Naval Weapons Center. Metal Particle Combustion Progress Report, 1 July 1965-1 May 1967, by Metal Combustion Study Group, edited by J. L. Prentice. China Lake, Calif., NWC, August 1968. 118 pp. (NWC TP 4435), UNCLASSIFIED.
35. U. S. Naval Ordnance Test Station. Aluminum Particle Combustion Progress Report, 1 April 1964-30 June 1965, by The Metal Combustion Study Group. China Lake, Calif., NOTS, April 1966. 116 pp. (TPR 415; NOTS TP 3916), UNCLASSIFIED.
36. Beckstead, M. W., and E. W. Price. Nonacoustic Combustor Instability, AMER INST AERONAUT ASTRONAUT J, Vol. 5, No. 11 (November 1967), pp. 1989-96.
37. Beckstead, M. W. Low Frequency Instability: A Comparison of Theory and Experiment, COMBUST AND FLAME, Vol. 12, No. 1 (October 1968), pp. 417-26.
38. Boggs, T. L., M. W. Beckstead, and O. H. Madden. The Effect of Oxidizer Particle Size and Binder Type on Nonacoustic Instability, New York, N. Y., American Institute of Aeronautics and Astronautics, 1969. AIAA Paper No. 69-175. 7 pp.
39. Culick, F. E. C. A Review of Calculations for Unsteady Burning of a Solid Propellant, AMER INST AERONAUT ASTRONAUT J, Vol. 6, No. 12 (December 1968), pp. 2241-55.
40. Sehgal, R., and L. Strand. A Theory of Low-Frequency Combustion Instability in Solid Rocket Motors, AMER INST AERONAUT ASTRONAUT J, Vol. 2, No. 4 (April 1964), pp. 696-702.
41. Coates, R. L., N. S. Cohen, and L. R. Harvill. An Interpretation of L^* Combustion Instability in Terms of Acoustic Instability Theory, AMER INST AERONAUT ASTRONAUT J, Vol. 5, No. 6 (June 1967), pp. 1097-1102.
42. Beckstead, M. W., N. Ryan, and A. D. Baer. Non-Acoustic Instability of Composite Propellant Combustion, AMER INST AERONAUT ASTRONAUT J, Vol. 4, No. 9 (September 1966), pp. 1622-28.

43. Oberg, S. L. Combustion Instability: The Relationship Between Acoustic and Nonacoustic Instability, AMER INST AERONAUT ASTRONAUT J, Vol. 6, No. 2 (February 1968), pp. 265-71.
44. T'ien, J. S., Sirignano, W. A., and M. Summerfield. Theory of L-star Combustion Instability with Temperature Oscillations, AIAA 6th Aerospace Sciences Meeting, New York, N. Y., January 1968. (AIAA Paper No. 68-179).
45. Culick, F. E. C. Some Nonscoustic Instabilities in Rocket Chambers Are Acoustic, Technical Notes, AMER INST AERONAUT ASTRONAUT J, Vol. 6, No. 7 (July 1968), pp. 1421-23.
46. Beckstead, M. W., H. E. Mathes, E. W. Price, and P. E. C. Culick. Combustion Instability of Solid Propellants, in "twelfth Symposium (International) on Combustion." Pittsburgh, Pa., Combustion Institute, 1968. Pp. 0011-0019.
47. Naval Weapons Center. Experimental Studies on the Oscillatory Combustion of Solid Propellants, by Aerothermochemistry Division. China Lake, Calif., NWC, March 1969. 108 pp. (NWC TP 4393), UNCLASSIFIED.
48. U. S. Naval Ordnance Test Station. Testing the Dynamic Stability of Solid Propellants: Techniques and Data, by M. D. Horton. China Lake, Calif., NOTS, August 1964. 50 pp. (NAVWEPS Report 8596, NOTS TP 3610), UNCLASSIFIED.
49. Horton, M. D., J. L. Eisel, and E. W. Price. Low-Frequency Acoustic Oscillatory Combustion, AMER INST AERONAUT ASTRONAUT J, Vol. 1, No. 11 (November 1963), pp. 2652-54.
50. Mathes, H. B., and E. W. Price. Measurement of Combustion Dynamics of Solid Propellants in the Low Frequency Range, New York, N. Y., American Institute of Aeronautics, 1967. AIAA Paper No. 67-70. 7 pp.
51. Eisel, J. L., M. D. Horton, E. W. Price, and D. W. Rice. Preferred Frequency Oscillatory Combustion of Solid Propellants, AMER INST AERONAUT ASTRONAUT J, Vol. 2, No. 7 (July 1964), pp. 1319-23.
52. Krier, H., J. S. T'ien, W. A. Sirignano, and M. Summerfield. Non-steady Burning Phenomena of Solid Propellants: Theory and Experiments, AMER INST AERONAUT ASTRONAUT J, Vol. 6, No. 2 (February 1968), pp. 278-85.
53. U. S. Naval Ordnance Test Station. Acoustic Tests of NASA 260-Inch Diameter, Solid Rocket Motor Models, by F. G. Buffum, D. R. Skar, P. H. Werback, and E. W. Price. China Lake, Calif., NOTS, June 1967. 18 pp. (NOTS Technical Note 508-47), UNCLASSIFIED.

54. Price, E. W. Recent Advances in Solid Propellant Combustion Instability, in "Twelfth Symposium (International) on Combustion." Pittsburgh, Pa., Combustion Institute, 1968.

UNCLASSIFIED

Security Classification

DOCUMENT CONTROL DATA - R&D		
<i>(Security classification of title, body of abstract and indexing annotation must be entered when the overall report is classified)</i>		
1. ORIGINATING ACTIVITY (Corporate author) Naval Weapons Center China Lake, California 93555		2a. REPORT SECURITY CLASSIFICATION UNCLASSIFIED
		2b. GROUP
3. REPORT TITLE COMBUSTION OF SOLID PROPELLANTS AND LOW FREQUENCY COMBUSTION INSTABILITY PROGRESS REPORT, 1 OCTOBER 1967-1 NOVEMBER 1968		
4. DESCRIPTIVE NOTES (Type of report and inclusive dates) PROGRESS REPORT, 1 October 1967-1 November 1968		
5. AUTHOR(S) (Last name, first name, initial) Boggs, T. L.; Mathea, H. B.; Price, E. W.; Kraeutle, K. J.; Dehority, G. L.; Crump, J. E.; and Culick, W. E. C.		
6. REPORT DATE June 1969	7a. TOTAL NO. OF PAGES 68	7b. NO. OF REFS 54
8a. CONTRACT OR GRANT NO.		9a. ORIGINATOR'S REPORT NUMBER(S)
a. PROJECT NO. NASA Work Order No. 6050		NWC TR 4749
c.		9b. OTHER REPORT NO(S) (Any other numbers that may be assigned to this report)
d.		
10. AVAILABILITY/LIMITATION NOTICES This document is subject to special export controls and each transmittal to foreign governments or foreign nationals may be made only with prior approval of the Naval Weapons Center.		
11. SUPPLEMENTARY NOTES		12. SPONSORING MILITARY ACTIVITY Naval Ordnance Systems Command Department of the Navy Washington, D. C. 20360
13. ABSTRACT → This report summarizes studies of ammonium perchlorate deflagration; one-dimensional modeling of steady-state burning; burning rate behavior of propellants with bimodal oxidizer particle size distribution; burning surface structure; and mechanism of metal agglomeration on burning surfaces. A review is presented of the status of knowledge of bulk mode instability. Brief sum- maries are presented of other recently published work, including (1) extension of one-dimensional combustion perturbation models to treat transient gas phase response, (2) collection of response function data from three different experi- mental techniques to present a full range map of μ/τ versus f and f for pro- pellants, and (3) further experimental studies of the structure of the combus- tion zone. <i>C.R.</i> <i>Small perturbation/pressure perturbation</i> <i>frequency</i>		

DD FORM 1 JAN 64 1473 0101-307-3800

UNCLASSIFIED

Security Classification

14. KEY WORDS	LINK A		LINK B		LINK C	
	ROLE	WT	ROLE	WT	ROLE	WT
Combustion Propellant Instability Rocket						

INSTRUCTIONS

1. **ORIGINATING ACTIVITY:** Enter the name and address of the contractor, subcontractor, grantee, Department of Defense activity or other organization (*corporate author*) issuing the report.
2. **REPORT SECURITY CLASSIFICATION:** Enter the overall security classification of the report. Indicate whether "Restricted Data" is included. Marking is to be in accordance with appropriate security regulations.
- 2b. **GROUP:** Automatic downgrading is specified in DoD Directive 5200.10 and Armed Forces Industrial Manual. Enter the group number. Also, when applicable, show (but optional) markings have been used for Group 3 and Group 4 as authorized.
3. **REPORT TITLE:** Enter the complete report title in all capital letters. Titles in all cases should be underlined. If a meaningful title cannot be selected without classification, show title classification in all capitals in parentheses immediately following the title.
4. **DESCRIPTIVE NOTES:** If appropriate, enter the type of report, e.g., interim, progress, summary, annual, or final. Give the inclusive dates when a specific reporting period is covered.
5. **AUTHOR(S):** Enter the name(s) of author(s) as shown on or in the report. Enter last name, first name, middle initial. If military, show rank and branch of service. The name of the principal author is an absolute minimum requirement.
6. **REPORT DATE:** Enter the date of the report as day, month, year, or month, year. If more than one date appears on the report, see date of publication.
- 7a. **TOTAL NUMBER OF PAGES:** The total page count should follow normal pagination procedure, i.e., enter the number of pages containing information.
- 7b. **NUMBER OF REFERENCES:** Enter the total number of references cited in the report.
- 8a. **CONTRACT OR GRANT NUMBER:** If appropriate, enter the applicable number of the contract or grant under which the report was written.
- 8b, c, & d. **PROJECT NUMBER:** Enter the appropriate military department identification, such as project number, subproject number, system number, task number, etc.
- 9a. **ORIGINATOR'S REPORT NUMBER(S):** Enter the official report number by which the document will be identified and controlled by the originating activity. This number must be unique to this report.
- 9b. **OTHER REPORT NUMBER(S):** If the report has been assigned any other report number (either by the originator or by the sponsor), also enter this number(s).
10. **AVAILABILITY/LIMITATION NOTICES:** Enter any limitations on further dissemination of the report, other than those

imposed by security classification, using standard statements such as:

- (1) "Qualified requesters may obtain copies of this report from DDC."
- (2) "Foreign announcement and dissemination of this report by DDC is not authorized."
- (3) "U. S. Government agencies may obtain copies of this report directly from DDC. Other qualified DDC users shall request through _____."
- (4) "U. S. military agencies may obtain copies of this report directly from DDC. Other qualified users shall request through _____."
- (5) "All distribution of this report is controlled. Qualified DDC users shall request through _____."

If the report has been furnished to the Office of Technical Services, Department of Commerce, for sale to the public, indicate this fact and enter the price, if known.

11. **SUPPLEMENTARY NOTES:** Use for additional explanatory notes.
12. **SPONSORING MILITARY ACTIVITY:** Enter the name of the departmental project office or laboratory sponsoring (paying for) the research and development. Include address.
13. **ABSTRACT:** Enter an abstract giving a brief and factual summary of the document indicative of the report, even though it may also appear elsewhere in the body of the technical report. If additional space is required, a continuation sheet shall be attached.

It is highly desirable that the abstract of classified reports be unclassified. Each paragraph of the abstract shall end with an indication of the military security classification of the information in the paragraph, represented as (TS), (S), (C), or (U).

There is no limitation on the length of the abstract. However, the suggested length is from 150 to 225 words.

14. **KEY WORDS:** Key words are technically meaningful terms or short phrases that characterize a report and may be used as index entries for cataloging the report. Key words must be selected so that no security classification is required. Identifiers, such as equipment model designation, trade name, military project code name, geographic location, may be used as key words but will be followed by an indication of technical context. The assignment of title, rates, and weights is optional.